Development/Plasticity/Repair

Fascin Regulates the Migration of Subventricular Zone-Derived Neuroblasts in the Postnatal Brain

Martina Sonego,[1] Sangeetha Gajendra,[1] Maddy Parsons,[2] Yafeng Ma,[3] Carl Hobbs,[1] Marc P. Zentar,[1] Gareth Williams,[1] Laura M. Machesky,[3] Patrick Doherty,[1] and Giovanna Lalli[1]

[1]Wolfson Centre for Age-Related Diseases, and [2]Randall Division, King's College London, Guy's Campus, London SE1 1UL, United Kingdom, and [3]Beatson Institute for Cancer Research, Glasgow University College of Medical, Veterinary and Life Sciences, Garscube Estate, Bearsden, Glasgow G61 1BD, United Kingdom

After birth, stem cells in the subventricular zone (SVZ) generate neuroblasts that migrate along the rostral migratory stream (RMS) to become interneurons in the olfactory bulb (OB). This migration is a fundamental event controlling the proper integration of new neurons in a pre-existing synaptic network. Many regulators of neuroblast migration have been identified; however, still very little is known about the intracellular molecular mechanisms controlling this process. Here, we show that the actin-bundling protein fascin is highly upregulated in mouse SVZ-derived migratory neuroblasts. *Fascin-1ko* mice display an abnormal RMS and a smaller OB. Bromodeoxyuridine labeling experiments show that lack of fascin significantly impairs neuroblast migration, but does not appear to affect cell proliferation. Moreover, fascin depletion substantially alters the polarized morphology of rat neuroblasts. Protein kinase C (PKC)-dependent phosphorylation of fascin on Ser39 regulates its actin-bundling activity. *In vivo* postnatal electroporation of phosphomimetic (S39D) or nonphosphorylatable (S39A) fascin variants followed by time-lapse imaging of brain slices demonstrates that the phospho-dependent modulation of fascin activity ensures efficient neuroblast migration. Finally, fluorescence lifetime imaging microscopy studies in rat neuroblasts reveal that the interaction between fascin and PKC can be modulated by cannabinoid signaling, which controls neuroblast migration *in vivo*. We conclude that fascin, whose upregulation appears to mark the transition to the migratory neuroblast stage, is a crucial regulator of neuroblast motility. We propose that a tightly regulated phospho/dephospho-fascin cycle modulated by extracellular signals is required for the polarized morphology and migration in neuroblasts, thus contributing to efficient neurogenesis.

Introduction

The subventricular zone (SVZ) is one of the main neurogenic niches in the postnatal brain (Doetsch et al., 1999; Alvarez-Buylla and Lim, 2004). SVZ stem cell-derived neural progenitors migrate along the rostral migratory stream (RMS) toward the olfactory bulb (OB), where they differentiate into GABAergic interneurons (Luskin, 1993; Lois and Alvarez-Buylla, 1994; Lledo et al., 2006). These migrating progenitors also have the ability to reach injured areas (Curtis et al., 2007). Moreover, neuroblast streams directed toward the OB are likely to play an important role in infant human brain development (Sanai et al., 2011).

ECM components (Blake et al., 2008), cell adhesion molecules (Chazal et al., 2000; Belvindrah et al., 2007), growth factors (Zhang et al., 2003; Snapyan et al., 2009), axon guidance receptors (Conover et al., 2000; Nguyen-Ba-Charvet et al., 2002; Kaneko et al., 2010; Saha et al., 2012), and neurotransmitters (Lledo et al., 2006; Pathania et al., 2010) regulate neuroblast migration. We also recently showed that an endocannabinoid (eCB) tone controls the polarized morphology and motility of RMS neuroblasts (Oudin et al., 2011b). However, how these signals couple to the intracellular machinery to control migration is still not understood. Since disrupting migration affects neuronal maturation (Belvindrah et al., 2011), uncovering the molecular players involved in this process is essential to understand the link between neurogenesis and plasticity and to exploit the therapeutic potential of stem cell-derived neural progenitors.

Here, we investigated the function of the actin-binding protein fascin in the postnatal SVZ/RMS. Fascin organizes actin filaments into parallel bundles (Adams, 2004), contributing to protrusion dynamics in cell adhesion, interaction, and motility (Kureishy et al., 2002; Vignjevic et al., 2003; Adams, 2004; Zanet et al., 2009; Jayo and Parsons, 2010; Jayo et al., 2012). It is highly expressed in the nervous system during embryonic development (De Arcangelis et al., 2004) and promotes filopodia stability, favoring growth cone extension (Cohan et al., 2001; Yamakita et al., 2009). Dynamic modulation of fascin-dependent actin bundling modulates growth cone collapse and reorientation (Cohan et al., 2001; Brown and Bridgman, 2009; Deinhardt et al., 2011). Phosphorylation on Ser39 by protein kinase C (PKC) reduces the

Received Feb. 12, 2013; revised May 17, 2013; accepted June 8, 2013.

Author contributions: M.S., M.P., P.D., and G.L. designed research; M.S., S.G., M.P., Y.M., C.H., and M.P.Z. performed research; L.M.M. and P.D. contributed unpublished reagents/analytic tools; M.S., S.G., M.P., Y.M., G.W., and G.L. analyzed data; M.S. and G.L. wrote the paper.

This work was supported by a Wellcome Trust Project grant (089236/Z/09/Z) awarded to P.D. and G.L. M.S. and S.G. were supported by King's College London and Biotechnology and Biological Sciences Research Council PhD studentships. Y.M. and L.M.M. are supported by a Cancer Research UK core grant. We thank Francis Szele for valuable advice on experimental protocols; Masaru Okabe for providing pCX-EGFP; and Mustafa Duman for help with time-lapse imaging analysis. We thank Matt Grubb and Brian Stramer for valuable comments on the manuscript.

Correspondence should be addressed to Dr. Giovanna Lalli, The Wolfson Centre for Age-Related Diseases, The Wolfson Wing, Hodgkin Building, King's College London, Guy's Campus, London SE1 1UL, United Kingdom. E-mail: giovanna.lalli@kcl.ac.uk.

DOI:10.1523/JNEUROSCI.0653-13.2013

 0270-6474/13/3312171-15$15.00/0

ability of fascin to bundle actin filaments (Yamakita et al., 1996) and regulates adhesion in a variety of metastastic cancer cells, where it also influences invadopodia and podosome stability (Li et al., 2010; Hashimoto et al., 2011). Fascin is upregulated in neuroectodermal progenitors derived from cultured human embryonic stem cells (Chae et al., 2009), but its function in neurogenesis is unknown. *Fascin-1ko* mice seem to lack major developmental defects (Yamakita et al., 2009). We discover that fascin is upregulated in RMS migratory neuroblasts. *Fascin-1ko* mice display an abnormal RMS, a smaller OB, and impaired neuroblast migration. We show that dynamic PKC-dependent fascin phosphorylation controls neuroblast motility using RMS explants, *in vivo* postnatal electroporation, and time-lapse microscopy. Fluorescence lifetime imaging microscopy (FLIM) studies reveal that cannabinoid signaling influences the PKC–fascin interaction in migrating neuroblasts. Thus, a fine control of fascin phosphorylation/dephosphorylation ensures proper neurogenesis by controlling neuroblast migration in the postnatal brain.

Materials and Methods

Reagents

Cell culture reagents were from Invitrogen, and all other reagents were from Sigma if not otherwise specified. Antibodies used were as follows: mouse anti-fascin and rabbit anti-GFAP (Dako); mouse anti-bromodeoxyuridine (BrdU) and rabbit anti-PKCα (BD Biosciences); rabbit anti-βIII-tubulin, anti-doublecortin (Dcx), and anti-Mash1 (Abcam); rabbit anti-GFP (Invitrogen); and rabbit anti-PKCγ (Santa Cruz Biotechnology). Alexa Fluor 488-phalloidin, Texas Red-X, or Alexa Fluor 488-conjugated anti-rabbit or anti-mouse IgG were from Invitrogen.

Animals

Sprague Dawley P6–P7 rat pups (Harlan) and P2 CD-1 mouse pups (Charles River) of either sex were used. All procedures were performed in accordance with UK Home Office Regulations (Animal Scientific Procedures Act, 1986).

The generation of *fascin-1* knock-out mice has been previously described (Yamakita et al., 2009). Briefly, the *fascin-1* gene is disrupted by a retrovirus insertion at the level of the intron between exon 1 and exon 2. For all experiments with homozygous knock-out mice, their wild-type (wt) littermates were used as a control. Brains from early postnatal (P7) and adult (P50) wt and *fascin-1ko* mice were used.

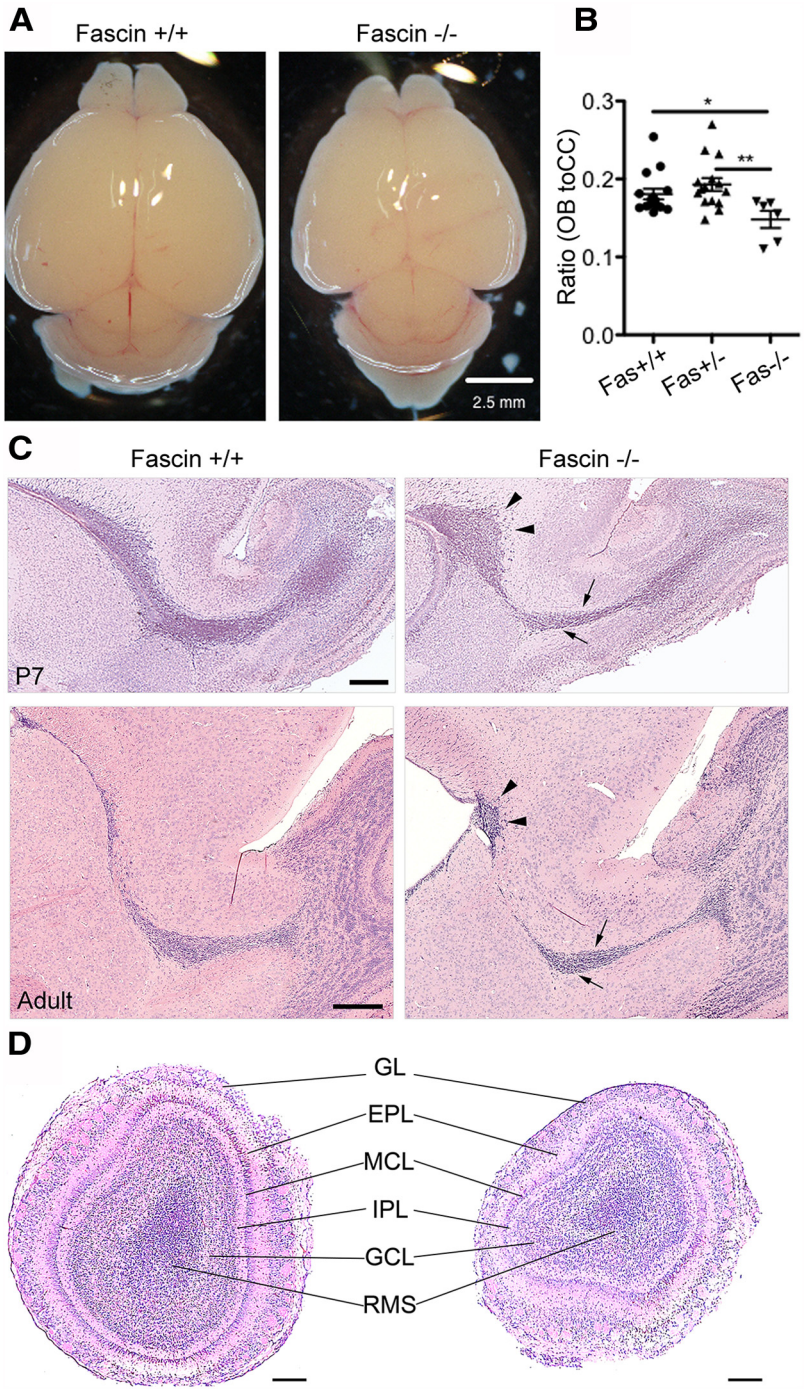

Figure 1. *Fascin-1ko* mice show a smaller OB and an abnormal RMS organization. ***A***, ***B***, Early postnatal (P7) homozygous *fascin-1ko* mice have a smaller brain (***A***) and a lower ratio between OB and cerebral cortex (CC) length (***B***) compared with wt and heterozygous littermates (mean ± SEM; $n = 15$ brains for wt and heterozygous *fascin-1ko*; $n = 6$ brains for homozygous *fascin-1ko*; $^*p < 0.05$; $^{**}p < 0.01$). ***C***, Hematoxylin/eosin-stained sagittal brain slices from P7 (top row) and P50 (bottom row) mice showing abnormal RMS organization in *fascin-1ko* animals. Note the thinner RMS rostral section (arrows) and a caudal cell accumulation (arrowheads). ***D***, Hematoxylin/eosin-stained coronal OB sections in P7 mice. The general organization of the OB appears preserved in *fascin-1ko* animals. GL, Glomerular layer; EPL, external plexiform layer; MCL, mitral cell layer; IPL, internal plexiform layer; GCL, granule cell layer. Scale bars: ***A***, 2.5 mm; ***C***, ***D***, 200 μm.

Bromodeoxyuridine injections

To examine proliferation, a cohort of mice received one intraperitoneal injection of 50 mg/kg BrdU 2 h before perfusion and killing ($n = 5$ for both wt and *fascin-1ko*). To examine migration, another cohort received three intraperitoneal BrdU injections (50 mg/kg) per day for 3 consecutive days and was killed 12 d after the last injection ($n = 4$ for wt mice; $n = 3$ for *fascin-1ko* mice; Comte et al., 2011). Immunohistochemical detection of BrdU was performed as previously described (Goncalves et al., 2008). For proliferation analysis, we counted all BrdU+ cells found in a 500-μm-long and 40-μm-wide section of the lateral SVZ. A cell count was performed in at least seven evenly spaced sections per animal, from coordinates 0.02–1.33 relative to bregma. For migration analysis, a square outline (covering a total area of 400 μm^2) was superimposed on confocal projection images of the caudal RMS and the core of the OB obtained from 35-μm-thick sagittal slices.

Cell counts in the square areas were performed in four slices per brain to calculate the relative percentages of cells found in the two areas.

RMS explant migration assay

RMS explants were dissected from P6/P7 Sprague Dawley rat pups, as previously described (Ward and Rao, 2005), and mixed with growth factor-reduced phenol red-free reconstituted extracellular matrix gel (Matrigel; Becton Dickinson) containing complete culture medium (2 mM L-glutamine, B27 supplement, and 0.6% glucose in Neurobasal medium) in a 3:1 ratio. The explant–Matrigel mix was spread over the surface of glass coverslips or four-chamber Hi-Q4 culture dishes (Nikon) and incubated at 37°C, 5% CO_2 for 5 min (or until the Matrigel began to solidify). Neurobasal complete medium was then added to maintain the explants at 37°C and 5% CO_2. Neuroblasts were left to migrate out of explants for 24 h before fixation.

Immunocytochemistry of Matrigel-embedded RMS explants

Coverslips were fixed in 4% paraformaldehyde (PFA) at room temperature for 40 min, washed with PBS, and blocked with 5% goat serum block (15% goat serum, 0.3% Triton X-100, and 1 mg/ml BSA in PBS) for 1 h at room temperature. They were then incubated with goat serum block containing fluorescent phalloidin for 2 h to stain F-actin, and subsequently with primary antibodies overnight at 4°C. After washing, coverslips were incubated for 2 h with secondary antibodies, Hoechst stained, and mounted using a mounting medium (Dako). Images of fixed explants were acquired using either an Axioplan 2 microscope equipped with a 10× or 20× objective (Carl Zeiss) or a Zeiss LSM 710 confocal microscope with 405, 488, and 594 nm lasers using 40× and 63× objectives. Pictures were processed using Adobe Photoshop.

Neuroblast nucleofection

Neuroblasts were obtained by trituration of P6/P7 rat RMS explants, as previously described (Oudin et al., 2011b). Cells were then either nucleofected (see below) or directly plated onto polyornithine and laminin-coated six-well plates or glass coverslips at a density of 1×10^6/well or $3–5 \times 10^4$/coverslip and maintained in complete culture medium at 37°C, 5% CO_2. Dissociated cells were suspended in rat neuron nucleofection solution (Lonza), mixed with 9 μg of short interfering RNA (siRNA) or 5 μg of plasmid DNA and nucleofected using program G13. A smart pool of four siRNA oligos targeting rat fascin (5′CCGACGAGAU CGCGGUAGA3′, 5′AGGCCUGCGCGGAGACUAU3′, 5′UGAGAGCGU CCAACGGCAA3′, 5′GUUCAAUGAUGGCGCCUAC3′) and control nontargeting siRNA (5′AGGUAGUGUAAUCGCCUUGTT3′) were used (Dharmacon). Cells were resuspended in DMEM + 10% FCS and reaggregated in hanging drops placed on the inner side of a 35 mm dish lid for 5 h at 37°C, 5% CO_2. Cell aggregates were then maintained in suspension in complete culture medium (over 24 or 52 h for DNA and siRNA nucleofections, respectively) before Matrigel embedding. Neuroblasts were allowed to migrate for 24 h at 37°C, 5% CO_2 before fixation. For morphological analysis, we counted the number of cells displaying secondary branching defined as a protrusion from the leading process of more than one somal length from the tip of the growth cone (to differentiate from a branched growth cone), as previously described (Koizumi et al., 2006; Oudin et al., 2011b). At least 150 cells were analyzed per condition in each of four independent experiments.

Fluorescence lifetime imaging microscopy

Rat neuroblasts were nucleofected with plasmids encoding monomeric RFP (mRFP)-tagged PKCα or PKCγ and GFP-fascin (Parsons and Adams, 2008), reaggregated and embedded in Matrigel 24 h after nucleofection. Cells were left to migrate for 9 h before adding drugs or CB agonists/antagonists to the culture medium for the indicated times, fixed in 4% PFA, incubated with 0.2% Triton X-100 in PBS for 10 min followed by 10 min quenching in 1% sodium borohydride, and mounted with Fluorsave (Calbiochem) for imaging. Multiphoton, time-correlated single-photon counting FLIM was performed to quantify interactions between protein pairs (PKCα/γ-mRFP and GFP-fascin) by fluorescence resonance energy transfer (FRET), as described previously. Briefly, a Nikon TE2000E inverted microscope combined with an in-house scanner and Chameleon Ti:Sapphire ultrafast pulsed multiphoton laser (Coherent) was used for excitation of GFP (at 890 nm). All images were acquired to provide enough photon arrival times to enable accurate fitting of fluorescence decay while avoiding detector pileup. Fluorescence lifetime imaging capability was provided by time-correlated single-photon counting electronics (SPC 700; Becker & Hickl). Widefield acceptor (mRFP) images were acquired using a CCD camera (Hamamatsu) at exposure times of <100 ms. Data were analyzed by performing a single-exponential pixel fit in TRI2 time-resolved image analysis software (developed by Dr. Paul Barber, Gray Institute, Oxford, UK). All histogram data are plotted as mean FRET efficiency from >10 cells/sample. Lifetime image examples shown are presented using a pseudocolor scale, whereby blue depicts normal GFP lifetime (i.e., no FRET) and red depicts reduced GFP lifetime (areas of FRET). Each experiment was repeated at least three times, and ANOVA was used to test statistical significance between different populations of data.

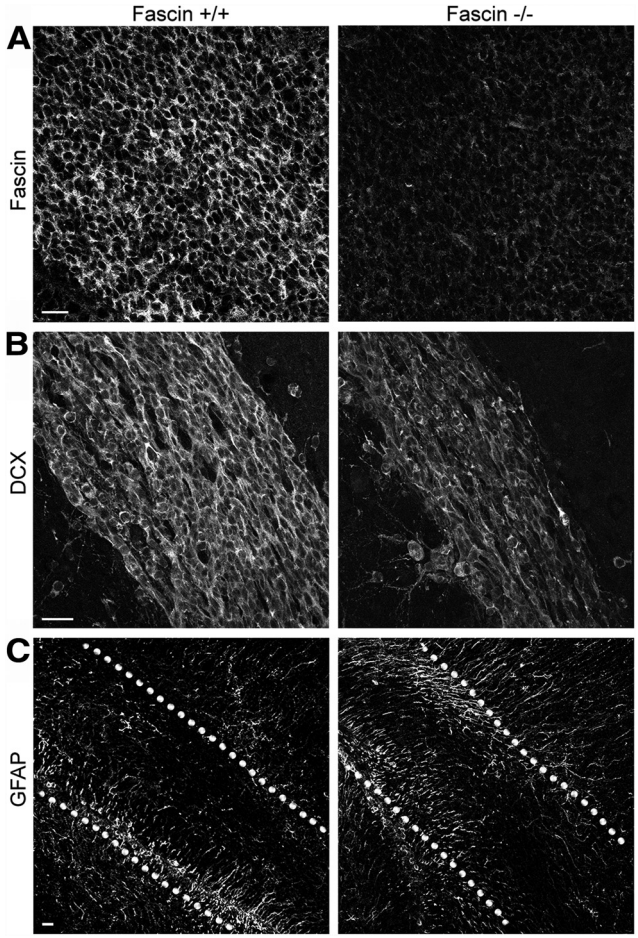

Figure 2. *Fascin-1ko* mice show abnormal neuroblast chain organization in the RMS. ***A***, Immunostaining of the SVZ/RMS in sagittal brain slices from P7 mice showing the absence of fascin in *fascin-1ko* animals. ***B***, Dcx-positive neuroblast chains appear thinner in *fascin-1ko* mice compared with wt mice. ***C***, Lack of fascin does not appear to perturb the localization of GFAP+ astrocytes and stem cells. The dotted lines outline the RMS borders. Scale bars: ***A***, ***B***, 20 μm; ***C***, 50 μm.

Postnatal in vivo *electroporation*

Electroporation was performed as previously described (Oudin et al., 2011b). Briefly, 3 μg of plasmid DNA (all at 1 μg/μl) were injected with a fine pulled glass capillary into the right lateral ventricle of P2 mouse pups anesthetized with isoflurane (0.6 L/min). pGFPC2-wt, S39A, and S39D fascin (Anilkumar et al., 2003) were coelectroporated with pCX-EGFP (a kind gift from M. Okabe, Osaka University, Osaka, Japan) at a 3:1 ratio to allow visualization by time-lapse spinning disk confocal microscopy. Animals were subjected to five electrical pulses of 99.9 V for 50 ms with 850 ms intervals using the CUY21SC electroporator (Nepagene) and 7 mm tweezer electrodes coated with conductive gel (Cefar). They

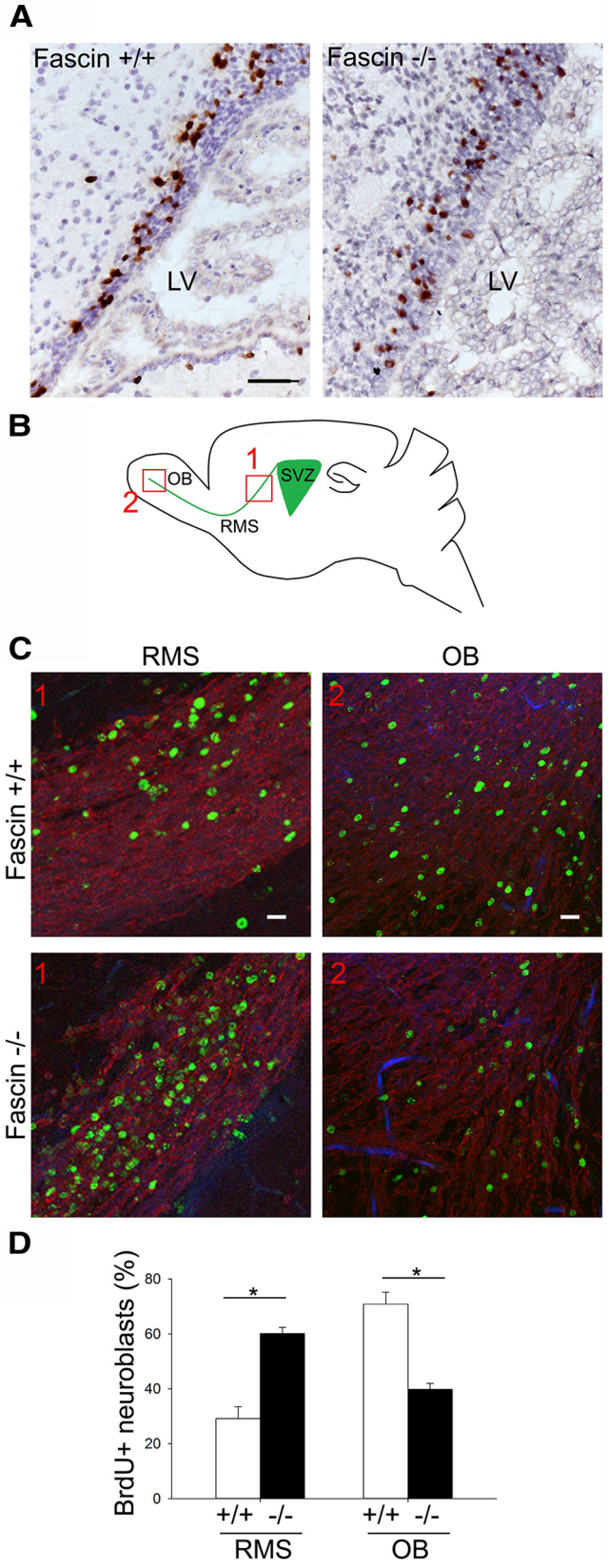

Figure 3. Genetic deletion of fascin affects neuroblast migration but not SVZ cell proliferation. ***A***, To analyze cell proliferation, 2 h after injecting wt and *fascin-1ko* mice with BrdU coronal brain sections were prepared for staining with anti-BrdU antibodies. Representative pictures showing BrdU+ cells in the SVZ (brown), showing no major difference in the amount of BrdU+ cells between wt and *fascin-1ko* samples. LV, Lateral ventricle. ***B***, To analyze SVZ-to-OB migration, P7 mice were injected with BrdU for 3 consecutive days. Twelve days later, sagittal brain slices were stained for Dcx and BrdU. Schematic diagram indicating the RMS/OB areas (areas 1 and 2) considered for quantification of BrdU+ cells. ***C***, Representative images of BrdU+ cells (green) in areas 1 and 2 of the RMS in wt and *fascin1-ko* mice. Sections were also stained for Dcx-labeled migrating neuroblasts (red). ***D***, *Fascin-1ko* animals display impaired migration, as shown by the increased percentage of BrdU+ cells in the caudal RMS and the decreased percentage of cells in the OB (mean ± SEM; $n = 4$ brains for wt mice; and $n = 3$ brains for *fascin-1ko* mice; $^*p < 0.05$). Scale bars: ***A***, 50 μm; ***C***, top, 1, 50 μm; ***C***, top, 2, 20 μm.

were reanimated under oxygen and returned to their mother. Brains were collected for immunohistochemical analysis or slice culture and videomicroscopy 5 d after electroporation.

Immunohistochemistry

Gelatin-embedded sections. After dissection, electroporated brains were kept in PBS containing 4% PFA at 4°C on a roller overnight before embedding in 4% gelatin and fixed again overnight in 4% PFA at 4°C. Brains were cut into 35-μm-thick sagittal slices using a Vibratome (VT10005; Leica). Slices were processed as previously described (Goncalves et al., 2008) before incubation with mouse anti-BrdU and rabbit anti-Dcx antibodies overnight at 4°C. After washing, slices were incubated with Alexa Fluor 488 anti-rabbit secondary antibody and Hoechst stained for 3 h at room temperature, washed again, and mounted. Confocal *z*-stacks were taken using a Zeiss LSM 710 microscope using 40× and 63× objectives.

Paraffin-embedded sections. Formalin-fixed P8 mouse brains were embedded in paraffin and cut into 6-μm-thick sagittal sections. Sections were deparaffinized and rehydrated before heat-induced antigen retrieval using a sodium citrate buffer. They were then blocked and incubated with primary antibodies overnight at 4°C. Biotinylated secondary antibodies (Vector Laboratories) were incubated at room temperature and detected with StreptABComplex/horseradish peroxidase (HRP; Vector Laboratories), and subsequently developed in DAB solution and counterstained with hematoxylin. Sections were dehydrated in 100% industrial methylated spirit, cleared in xylene, and mounted in DPX plastic.

An average of four to five sections per brain containing the full RMS was considered for morphological analysis. For immunofluorescence, sections were deparaffinized as previously described (Oudin et al., 2011b), blocked with 1% BSA for 15 min, and incubated overnight at 4°C with primary antibodies. Sections were then incubated with appropriate fluorescent secondary antibodies and/or Hoechst dye for 1 h at room temperature and mounted on slides using Mowiol.

Analysis of migration

Fixed RMS explants. Pictures of fixed explants were taken on an Apotome microscope (Zeiss) with 10× and 20× objectives. The migration distance was measured from the edge of the explants to the nucleus of the furthest migrated cell (identified by Hoechst staining) for at least six different positions around the explants by using ImageJ. The data generated were obtained from three independent experiments with at least 15 explants examined per condition for each experiment (Oudin et al., 2011b).

Time-lapse imaging of RMS explants. Time-lapse images of neuroblasts migrating out of RMS explants were acquired using a Nikon Biostation IM every 3 min for up to 24 h using a 20× objective in a controlled atmosphere (37°C, 5% CO_2). Videos were then tracked and analyzed using the Volocity 3D Image Analysis Software (PerkinElmer). Only isolated explants with a diameter >35 μm were considered. The nuclear movement of each cell was tracked for 7 h, and only cells that remained in focus during the 7 h period were examined. Seventy cells were tracked for each condition from a total of three independent experiments.

Time-lapse imaging of brain slices. Mouse pups were killed 5 d after electroporation. The electroporated right hemisphere was sliced into 300-μm-thick sagittal sections with a Vibratome (Leica). GFP-positive slices were cultured on a MilliCell insert (Millipore) submerged in imaging medium (1% glucose, B27 supplement, 2% L-glutamine, 10 mM HEPES, 1% Pen/Strep, and 5% FCS in phenol red-free DMEM) in a p35 dish for 1 h. The inserts were then transferred to a p35 glass-bottom dish

←

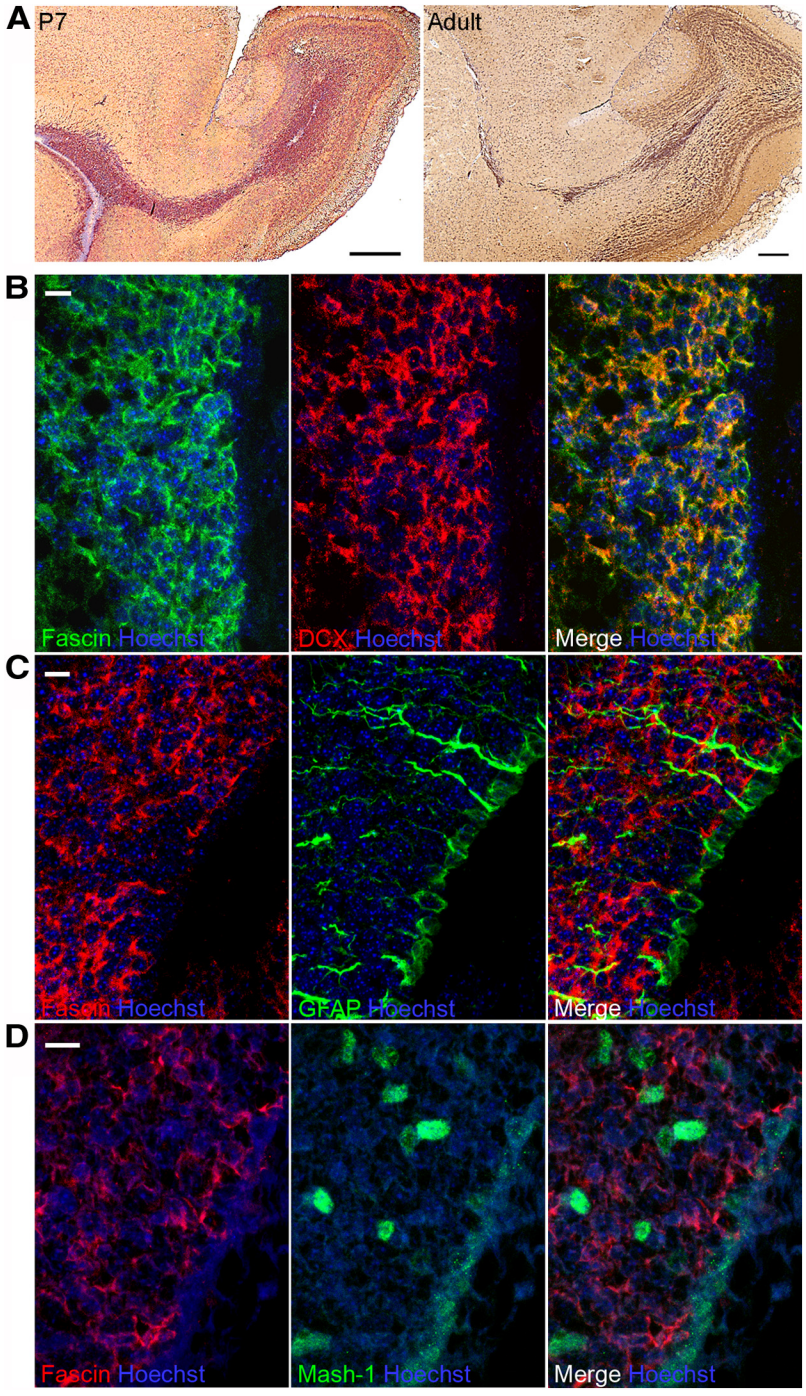

Figure 4. Fascin is upregulated in migrating neuroblasts. ***A***, Immunostaining of sagittal brain sections shows strong fascin expression along the RMS in both P7 and adult mice. ***B***, ***C***, Confocal images from P7 mouse SVZ sections showing that fascin immunostaining virtually overlaps with Dcx+ migrating neuroblasts (***B***), but is excluded from GFAP+ stem cells and astrocytes (***C***). ***D***, Hardly any colocalization is observed with Mash1+ transit-amplifying progenitors. Scale bars: ***A***, 500 μm; ***B–D***, 10 μm.

(MatTek), containing imaging medium. Confocal *z*-stack images (taken every 4 μm over an interval of 100–150 μm) of GFP-positive cells in the horizontal section after the RMS "elbow" were taken every 3 min for 3 h on a PerkinElmer UltraView VoX spinning disk system equipped with an inverted Nikon Ti-E microscope using a Nikon CFI Super Plan Fluor ELWD 20×/0.45 objective and a Hamamatsu Orca R2 camera. Movies were acquired and analyzed using the PerkinElmer Volocity software. For tracking analysis, only cells that were present within the imaging area for the entire duration of the movie and that moved over a total distance of at least 50 μm were analyzed. Between 15 and 30 cells were tracked for each slice, and at least 5 brains were analyzed for each electroporation. Branching events per hour were quantified by frame-by-frame visual analysis of time-lapse movies. For each condition, between 60 and 80 cells were analyzed from a total of six to eight brain slices per genotype.

Western blot analysis

Cells were scraped in lysis buffer (50 mM Tris, pH 8, 150 mM NaCl, 1 mM $CaCl_2$, 10 mM $MgCl_2$, 1% Triton X-100, 5% glycerol, 1 mM Na_3VO_4, 10 mM NaF, 1 mM PMSF, Protease inhibitor mix; Roche). Lysates were rotated for 30 min at 4°C and spun at 12,000 rpm for 10 min at 4°C. Supernatants were run on an 8% or 10% SDS-polyacrylamide gel and transferred onto Immobilon-P PVDF membranes (Millipore). After blocking in 5% nonfat dry milk in 0.1% Tween-20 in Tris buffered saline (TBS-T) for 1 h at room temperature, membranes were incubated overnight at 4°C with primary antibodies diluted in TBS-T/milk. Following washing in TBS-T, membranes were incubated with HRP-conjugated antibodies for 1 h at room temperature, washed, incubated with enhanced chemiluminescence Western Blotting reagent, and exposed to Hyperfilm (GE Healthcare).

Statistical analysis

Statistical analysis was performed using Student's *t* test for dual comparison and one-way ANOVA for multiple comparison with SigmaPlot 12.0 (SYSTAT). Differences were considered statistically significant if $p < 0.05$ (when shown, $^{*}p < 0.05$, $^{**}p < 0.01$, and $^{***}p < 0.001$).

Results

Genetic deletion of fascin affects RMS organization

At a gross level, *fascin-1ko* mice retain normal brain morphology apart from loss of the posterior region of the anterior commissure neuron and enlargement of the lateral ventricles (Yamakita et al., 2009). We noticed that these animals have lower body weight (at P7: wt, 3.81 ± 0.22 g, $n = 8$; heterozygous *fascin-1ko*, 3.92 ± 0.08 g, $n = 23$; homozygous *fascin-1ko*, 2.40 ± 0.19 g, $n = 6$) and a smaller brain compared with wt and heterozygous littermates (Fig. 1*A*). Moreover, the ratio between the length of the OB and the cerebral cortex is significantly decreased in *fascin-1ko* animals, indicating a specific reduction in OB size (Fig. 1*B*). We confirmed that *fascin-1ko* mice display an enlarged lateral ventricle, as previously reported (Yamakita et al., 2009). Closer inspection of hematoxylin/eosin-stained sagittal brain sections of these animals at an early postnatal stage (P7) revealed a thinner RMS compared with wt littermates (Fig. 1*C*, top row, arrows) and an abnormal cell accumulation in the caudal portion of the RMS (Fig. 1*C*, top row, arrowheads). These differences observed in the early postnatal brain were reflected in significant changes in the adult (P50) RMS morphology (Fig. 1*C*,

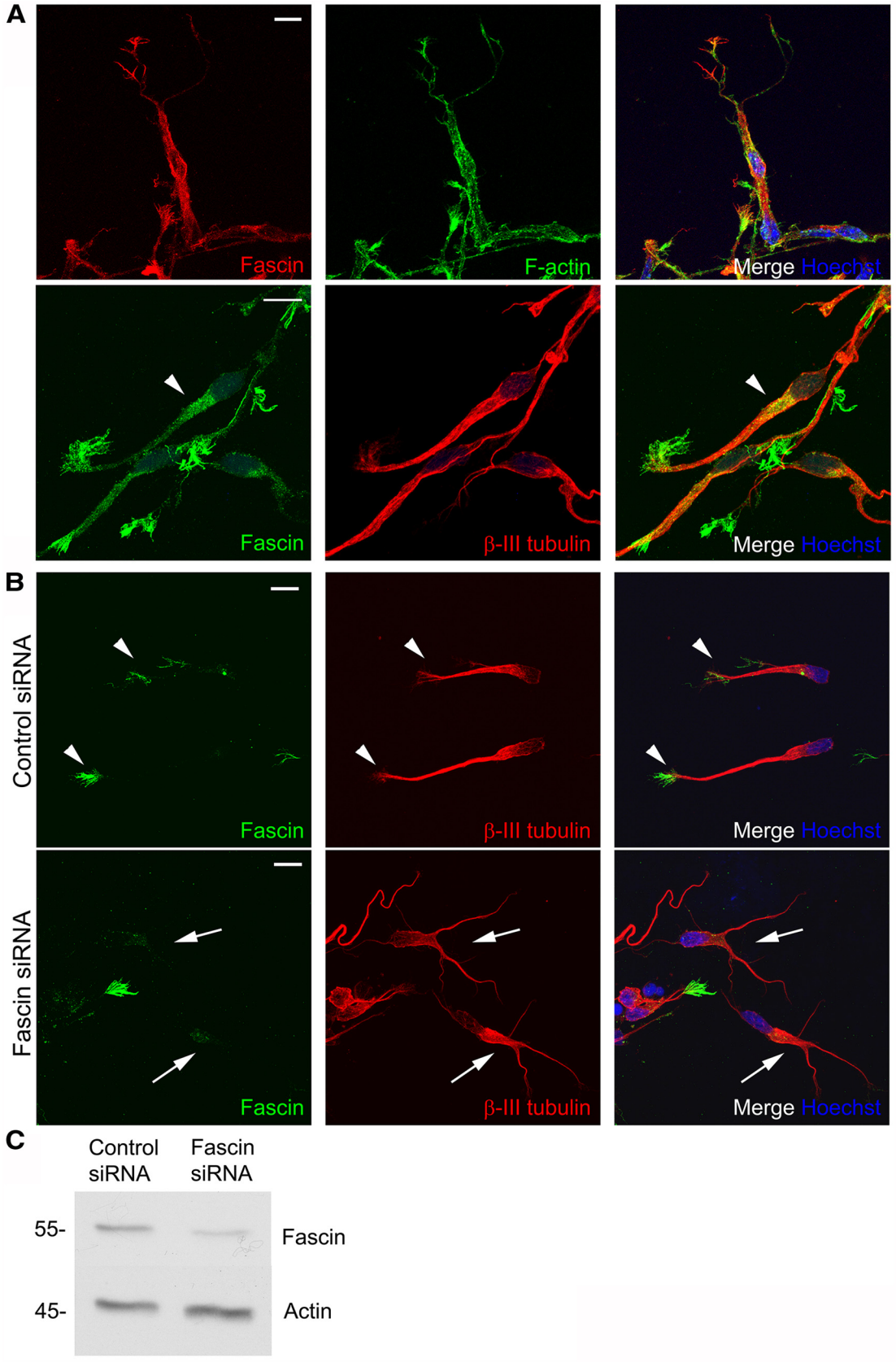

Figure 5. Fascin regulates neuroblast morphology. ***A***, Top row, Fascin (red) concentrates in peripheral filopodial structures (visualized by fluorescent phalloidin, green) in rat RMS neuroblasts migrating in Matrigel. Bottom row, Fascin immunoreactivity (green) can also be detected in front of the nucleus (arrowhead). Microtubules are stained by βIII-tubulin (red). ***B***, Rat neuroblasts were nucleofected with control or fascin siRNA, embedded in Matrigel 52 h after nucleofection, and left to migrate for 24 h before immunostaining for fascin (green) and the neuroblast marker βIII-tubulin (red). Top row, arrowheads, Control cells display a major leading process decorated with fascin at the leading edge. Bottom row, arrows, Fascin-depleted cells show branched, kinked protrusions. ***C***, Representative Western blot showing efficient fascin knockdown in neuroblasts 72 h after siRNA nucleofection. Scale bars: ***A***, ***B***, 10 μm.

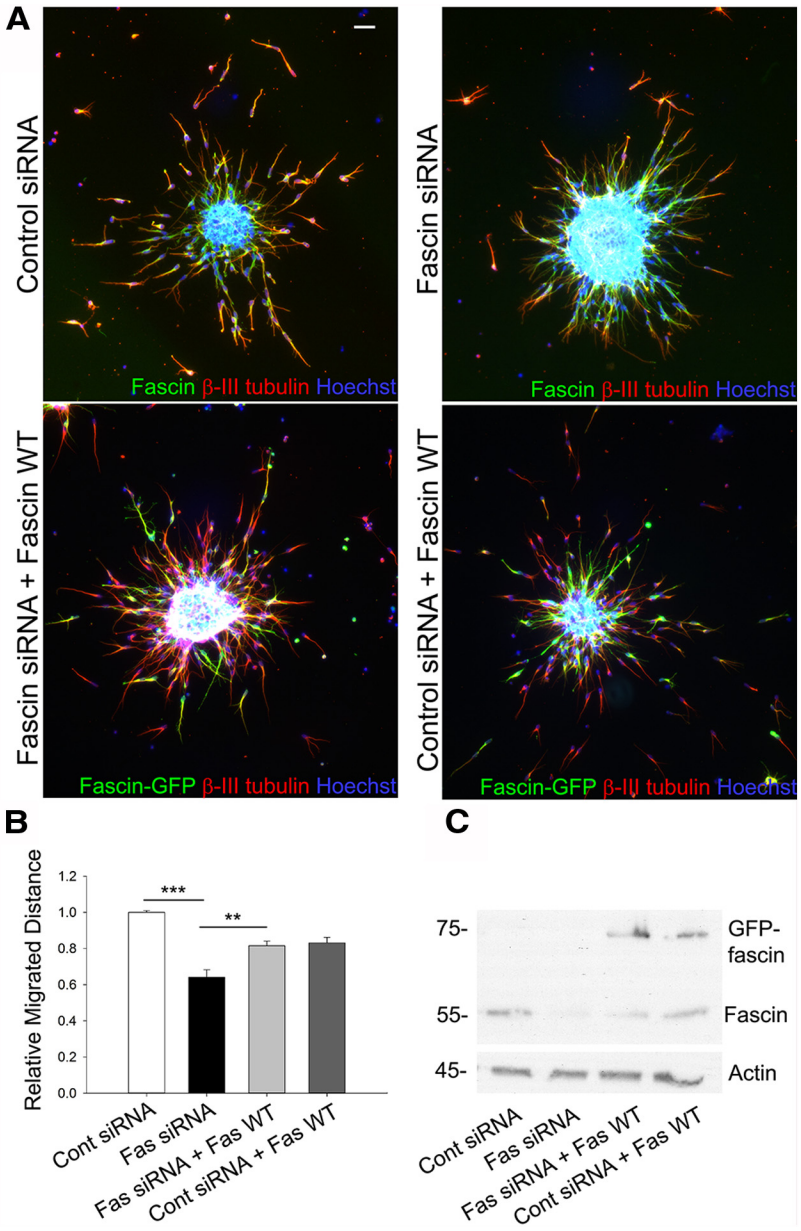

Figure 6. Fascin regulates neuroblast migration *in vitro*. ***A***, Reaggregated rat neuroblasts were embedded in Matrigel 52 h after nucleofection of control or fascin siRNA oligos with or without a GFP-tagged, siRNA-resistant wt human fascin, and were allowed to migrate for 24 h before immunostaining for fascin (green) and βIII-tubulin (red). Cell nuclei were visualized by Hoechst staining (blue). ***B***, Quantitative analysis shows a ~30% decrease of migration distance in fascin-depleted neuroblasts compared with cells nucleofected with control siRNA (mean ± SEM; $n = 3$; $^{**}p < 0.001$; $^{***}p < 0.001$). This effect is almost completely rescued by cotransfection with the siRNA-resistant wt fascin. ***C***, Western blot from nucleofected neuroblasts showing efficient fascin depletion and expression of GFP-wt fascin. Scale bar, 50 μm.

bottom row). Indeed, in adult brains the lack of fascin significantly decreased the width of the RMS elbow (wt, 149.673 ± 7.198 μm; *fascin-1ko*, 99.750 ± 6.396 μm; $n = 3$ brains/genotype, $p < 0.01$; Fig. 1*C*, bottom row, arrows), while still causing an abnormal cell accumulation in the caudal portion of the RMS (Fig. 1*C*, arrowheads; caudal RMS width: wt, 77.670 ± 4.342 μm; *fascin-1ko*, 118.800 ± 7.557 μm; $n = 3$ brains/genotype, $p < 0.01$). We did not detect evidence of ectopic neuroblast migration to other brain areas in *fascin-1ko* mice, which displayed an overall preserved OB structure (Fig. 1*D*). Fascin staining is absent in *fascin-1ko* brains (Fig. 2*A*), confirming the specificity of our immunostaining. In *fascin-1ko* mice, we noticed thinner Dcx-positive neuroblast chains and a weaker Dcx immunoreactivity along the RMS (Fig. 2*B*). In contrast, immunostaining for GFAP+ astrocytes and stem cells appeared similar to wt animals (Fig. 2*C*), suggesting that the lack of fascin affects RMS organization.

To investigate whether genetic deletion of fascin affects cell proliferation, we injected BrdU 2 h before analysis to label only actively proliferating cells in the SVZ and counted the BrdU+ cells along a section of the lateral SVZ (Fig. 3*A*). Care was taken to quantify cells at the same histological level in all animals. We could not detect any significant difference in the number of BrdU+ cells among wt, heterozygous, or homozygous *fascin-1ko* mice (wt, 59.09 ± 3.8; heterozygous *fascin-1ko*, 53.3 ± 1.8; homozygous *fascin-1ko*, 54.2 ± 5.6; $n = 5$ brains for each genotype).

To examine whether the lack of fascin impairs the migration of neuroblasts from the SVZ toward the OB, we injected mice with BrdU over a period of 3 d and killed them 12 d after the last injection (Comte et al., 2011). We counted BrdU+ cells in the caudal RMS and in the OB (Fig. 3*B*, areas 1 and 2), and calculated the percentage of cells found in these two areas. Compared with wt animals, *fascin-1ko* mice showed almost a 50% decrease in the percentage of cells reaching the OB, and a more than a doubled number of cells remaining in the RMS (Fig. 3*C*,*D*). Staining with antibodies against caspase 3 revealed only very few cells undergoing apoptosis, and there was no apparent increase in the number of caspase 3-positive cells in *fascin-1ko* mice (data not shown). Together, these results suggest that fascin deletion strongly impairs the migration of SVZ-derived neuroblasts.

Fascin depletion affects neuroblast morphology and motility

Given the abnormal RMS architecture observed in *fascin-1ko* mice, we decided to examine the localization of fascin in early postnatal and adult wt mouse brain sagittal slices. We found that fascin is highly expressed in the RMS in both cases (Fig. 4*A*). Double immunolabeling revealed a virtually complete colocalization of fascin with the migrating neuroblast marker Dcx (Fig. 4*B*), while no colocalization was observed with the astrocytic stem cell marker GFAP (Fig. 4*C*) and very little with Mash1, a transit amplifying progenitor marker (Fig. 4*D*), indicating that fascin expression is upregulated in migratory neuroblasts.

We further examined the spatial distribution and function of fascin in these cells using RMS explants embedded in a tridimensional Matrigel matrix to reproduce *in vitro* the typical neuroblast mode of migration observed *in vivo* (Wichterle et al., 1997). We found a strong fascin concentration along peripheral filopodia

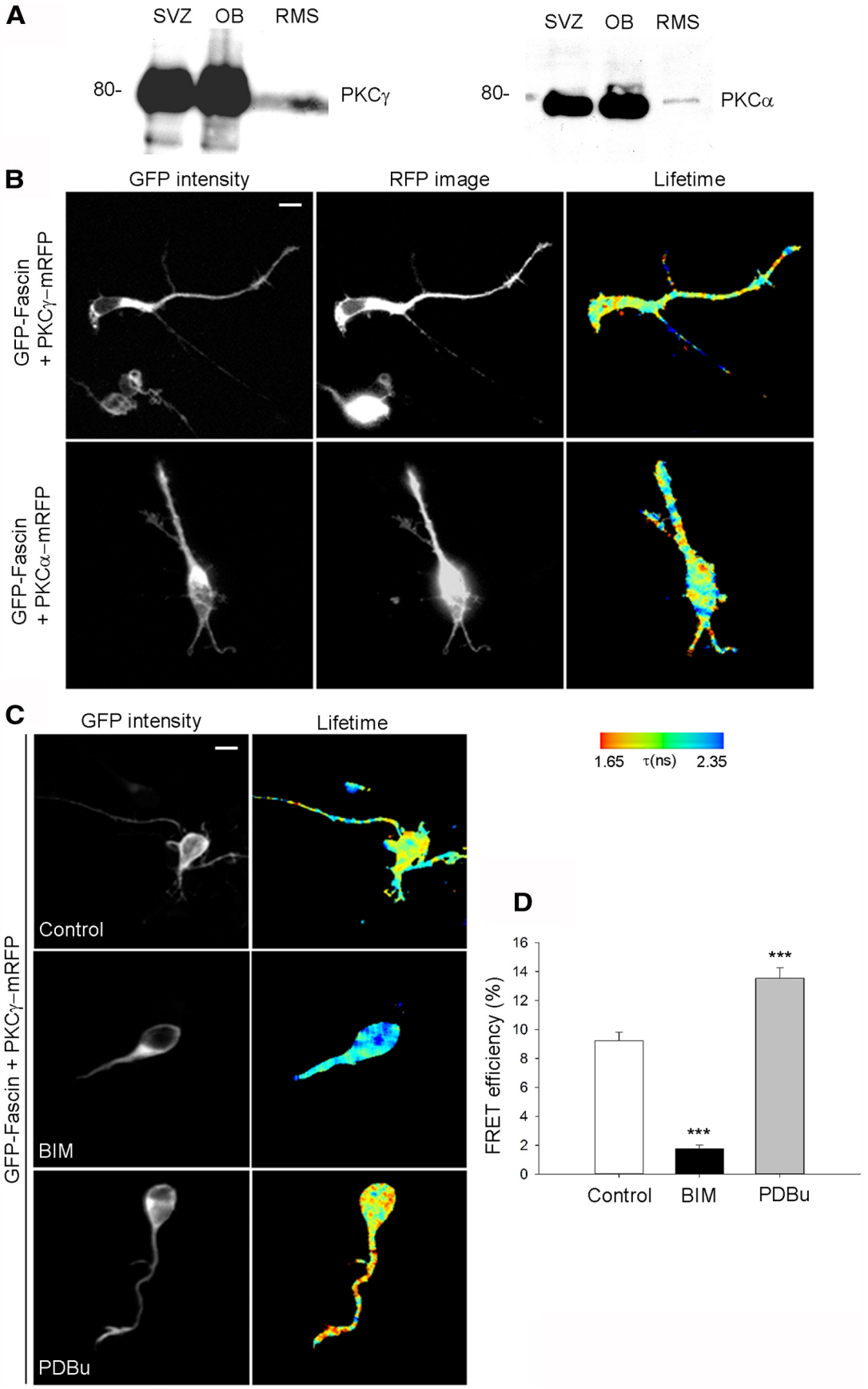

Figure 7. Interaction between fascin and PKCα or PKCγ can be detected by FLIM analysis in migrating neuroblasts. ***A***, PKCα and PKCγ are detected in the same Western blot of lysates from P7 rat SVZ, OB, and cultured RMS neuroblasts. ***B***, Rat neuroblasts expressing GFP-fascin and mRFP-tagged PKCα (top row) or PKCγ (bottom row) were fixed 24 h after nucleofection and imaged using FLIM to measure FRET efficiency. Each row shows images in the GFP channel (donor), RFP channel (acceptor). Lifetime (*Figure legend continues.*)

(Fig. 5*A*), and detected some fascin-positive immunostaining also along the leading process and especially ahead of the nucleus (Fig. 5*A*, bottom row, arrowhead), a site of F-actin condensation before nuclear translocation (Shinohara et al., 2012). To examine the functional role of fascin, we knocked it down by siRNA nucleofection. Cells were then reaggregated in a "hanging drop" (see Materials and Methods), cultured in suspension for 52 h, and subsequently embedded in Matrigel. Cells were left to migrate for 24 h before immunostaining for fascin and βIII-tubulin, a neuroblast marker. These conditions produced a very efficient fascin knockdown, which was confirmed both by immunocytochemistry and by Western blot (Fig. 5*B*,*C*). Fascin depletion dramatically affected neuroblast morphology. Many cells displayed multiple branching of the leading process or kinked protrusions compared with control cells, which instead showed a typical polarized, straight process (Fig. 5*B*). Quantitative analysis revealed almost a doubled percentage of branched cells after nucleofection of fascin siRNA compared with control siRNA (control siRNA, 24.901 ± 2.352; fascin siRNA, 42.230 ± 3.927; $p < 0.01$, $n = 150$ cells from four independent experiments).

Besides affecting the morphology of neuroblasts, knocking down fascin also impaired their migration (Fig. 6*A*). Quantitative analysis showed a ~30% decrease in migration distance for fascin-depleted cells compared with control neuroblasts (Fig. 6*B*). The defective migration was rescued by an siRNA-resistant GFP-tagged human fascin (Hashimoto et al., 2007), confirming the specificity of the siRNA effect (Fig. 6*A–C*). Quantitative tracking analysis of time-lapse imaging experiments over a period of 7 h revealed a significant decrease in speed and total migrated distance for the fascin-depleted cells, which also spent more time immobile (speed: control siRNA, 16.740 ± 0.756 μm/h; fascin siRNA, 13.738 ± 0.858 μm/h; $p < 0.01$; distance: control siRNA, 117.177 ± 5.295 μm; fascin siRNA, 96.163 ± 6.003 μm; $p < 0.01$; time spent immobile: control siRNA, 3.021 ± 0.105 h; fascin siRNA, 3.813 ± 0.122 h; $p < 0.001$, $n = 70$ cells from three independent experiments). Together, these results suggest that fascin regulates the polarized morphology and migration of neuroblasts.

Detecting fascin–PKC interaction in primary neuroblasts by FLIM

Following PKC-dependent phosphorylation on Ser39, fascin interacts with PKC, promoting migration in different cell types like myoblasts and colon carcinoma cells (Adams and Schwartz, 2000; Hashimoto et al., 2007). Both PKCα and PKCγ phosphorylate fascin on Ser39 (Ono et al., 1997; Parsons and Adams, 2008) and can be detected in lysates from RMS neuroblasts; however, PKCγ appears to be more abundant than PKCα, as shown by the same Western blot probe for PKCα and PKCγ (Fig. 7*A*). To monitor whether fascin and PKC interact in migrating neuroblasts, we adopted a FRET/FLIM approach using GFP-tagged fascin and PKCα or PKCγ tagged with mRFP (PKCα/γ-mRFP) as the donor and acceptor probes, respectively. FLIM allows precise spatial and temporal analysis of protein interaction in intact cells (Parsons et al., 2004; Worth and Parsons, 2010) and has been successfully used to monitor fascin–PKC interaction in non-neuronal cells (Anilkumar et al., 2003; Parsons and Adams, 2008). In standard culture conditions, we observed a higher degree of FRET efficiency for the fascin/PKCγ pair compared with the fascin/PKCα pair (Fig. 7*B*; fascin/PKCγ, 9.5000 ± 1.1851%; fascin/PKCα, 6.0667 ± 0.6391%; $n = 12$ cells for each condition), so we concentrated our subsequent studies on the analysis of the fascin–PKCγ interaction. We confirmed that this interaction depends on PKC activity by treating neuroblasts with 10 nM phorbol dibutyrate (PDBu) or 1 μM bisindolylmaleimide I (BIM) to directly activate or inhibit PKCγ activity, respectively (Parsons and Adams, 2008). Incubation with PDBu significantly increased FRET efficiency levels between GFP-fascin and PKCγ-mRFP, while BIM drastically decreased it, demonstrating that the fascin–PKCγ interaction depends on active PKCγ (Fig. 7*C*,*D*). These observations show that active PKC interacts with fascin in migratory neuroblasts and suggest that PKC-dependent Ser39 phosphorylation of fascin may have a functional role in their motility.

Fascin phosphorylation on Serine 39 regulates neuroblast migration

Phosphorylation of fascin on Ser39 inhibits its actin-bundling activity, modulating the balance between cell protrusions and adhesion (Ono et al., 1997; Anilkumar et al., 2003; Vignjevic et al., 2006). To assess the role of Ser39 phosphorylation in neuroblast migration, we nucleofected neuroblasts with three different GFP-tagged fascin variants: wt, phosphomimetic (S39D), or nonphosphorylatable (S39A; Anilkumar et al., 2003). Nucleofected cells were reaggregated overnight, embedded in Matrigel the following morning, and fixed 24 h later to analyze migration. Neuroblasts expressing wt fascin migrated similar to control cells expressing GFP (Fig. 8*A*,*B*). In contrast, an ~60% decrease in migration was observed for neuroblasts expressing either GFP-fascin S39D or GFP-fascin S39A (Fig. 8*A*,*B*). Importantly, nucleofection per se did not affect the ability of cells to migrate, since GFP-expressing cells migrated as well as "internal control" untransfected neuroblasts (Fig. 8*B*, hatched columns). Quantitative tracking analysis of time-lapse imaging experiments (Fig. 8*C–E*) showed that expressing either S39D or S39A fascin impaired neuroblast migration, decreasing total migrated distance by at least 30%, significantly lowering speed, and increasing the number of pauses compared with control cells. Together, these results strongly suggest that fascin phosphorylation on Ser39 regulates neuroblast migration.

Fascin phosphorylation regulates neuroblast directionality *ex vivo*

To investigate whether fascin phosphorylation on Ser39 affects neuroblast migration in the intact brain, we used *in vivo* postnatal electroporation, a technique allowing efficient transfection of SVZ-derived neuroblasts in the whole animal (Boutin et al., 2008; Oudin et al., 2011b). We coelectroporated empty vector, wt fascin, or fascin phosphomutants together with a GFP-expressing plasmid in the lateral ventricle of P2 mouse pups and monitored neuroblast migration by spinning disk confocal microscopy in acute brain slice cultures prepared 5 d after electroporation (Fig. 9*A*). Slices were imaged at 3 min intervals over a period of 3 h and subsequently analyzed using quantitative tracking. As reported earlier (Sawamoto et al., 2006; Hirota et al., 2007; Nam et al.,

←

(*Figure legend continued.*) images are depicted using a pseudocolor scale where red is a low GFP lifetime (high FRET) and blue is a high GFP lifetime (no FRET). ***C***, Rat neuroblasts expressing GFP-fascin and PKCγ-mRFP were treated with vehicle control, the PKC activator PDBu (10 nM, 10 min), or the PKC inhibitor BIM (1 μM, 15 min) 9 h after nucleofection; fixed; and analyzed using FLIM. Each row shows images in the GFP channel (donor) and pseudocolored lifetime images. ***D***, Activating PKC with PDBu enhances the fascin–PKCγ interaction as shown by the significant increase in FRET efficiency levels for the fascin/PKCγ pair, while inhibiting PKC with BIM severely reduces FRET efficiency (mean ± SEM; $n = 27$ cells for control; $n = 19$ cells for PDBu; and $n = 22$ cells for BIM from three independent experiments; ***$p < 0.001$). Scale bars: ***B***, ***C***, 5 μm.

2007; Bagley and Belluscio, 2010; Saha et al., 2012), we also observed cells in the RMS moving either forward (toward the OB) or backward (toward the SVZ), cells reversing their direction, cells remaining stationary, or cells moving locally (exploratory) during the imaging period. Overall, cells expressing wt, S39A, or S39D fascin tended to be more exploratory and less directed in their movement, as shown by a visual comparison of their trajectories (Fig. 9*B*). Quantitative tracking analysis (Fig. 9*C–E*) showed that, compared with control neuroblasts, cells expressing wt fascin migrated a slightly longer average distance, and had a higher average speed and similar displacement, intended as the shortest distance between start and stop points. In contrast, compared with control neuroblasts, cells expressing either S39A or S39D fascin migrated less, had a lower average speed, and were characterized by a shorter displacement. In addition, cells expressing the fascin phosphomutants branched more frequently (Fig. 10*A*,*B*) and were characterized by a more exploratory behavior, as shown by a decrease in their migratory index that is the ratio between net distance and total distance covered (Comte et al., 2011; Fig. 10*C*). The similar effects produced by the expression of both S39D and S39A fascin mutants strongly suggest that efficient neuroblast migration relies on a tightly regulated cycle between phospho- and dephosphofascin. Indeed, perturbing this delicate balance by overexpression of either phosphofascin mutant inevitably leads to motility and misorientation defects, causing cells to be slower, more branched, and less directed in their movement.

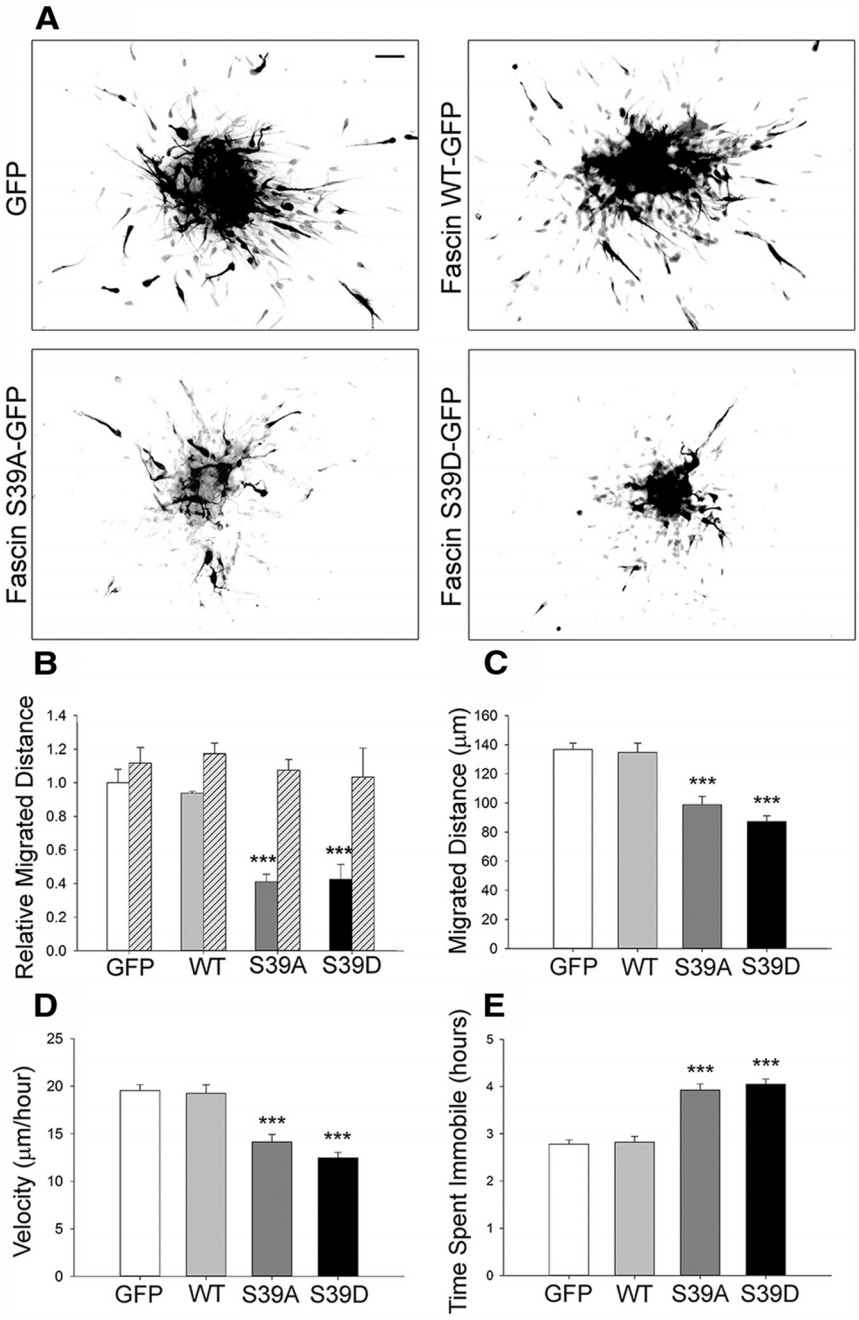

Figure 8. Phosphorylation of fascin on Ser39 regulates neuroblast migration *in vitro*. ***A***, Representative pictures of rat neuroblasts nucleofected with GFP, or GFP-tagged wt fascin, S39D fascin, or S39A fascin. The GFP channel is shown as a grayscale image. Reaggregated neuroblasts were embedded in Matrigel 24 h after nucleofection and allowed to migrate for 24 h. Expression of the two fascin phosphomutants visibly impairs migration. ***B***, Quantitative analysis from fixed samples shows an ~60% decrease in relative migration distance for neuroblasts expressing the fascin phosphomutants compared with control cells. The expression of wt fascin did not significantly affect migration. GFP-negative, untransfected cells served as an internal control (hatched columns; mean ± SEM; $n = 3$, $^{***}p < 0.001$). ***C–E***, Tracking quantitative analysis over a period of 7 h showing that neuroblasts expressing either S39A or S39D fascin migrate over shorter distances (***C***), are significantly slower (***D***), and spend more time immobile (***E***) compared with either GFP or wt fascin-expressing neuroblasts (mean ± SEM; $n = 70$ cells from three independent experiments; $^{***}p < 0.001$). Scale bar, 50 μm.

Cannabinoid signaling regulates the interaction between fascin and PKC in migrating neuroblasts

Our data point to an important role for fascin phosphorylation on Ser39 regulating neuroblast migration. Once phosphorylated on this residue, fascin is displaced from actin filaments and interacts with active PKC, contributing to proper cell adhesion to the extracellular matrix (Anilkumar et al., 2003). We therefore tested whether the fascin–PKC interaction can be modulated downstream of signals promoting neuroblast migration using the FLIM approach described earlier. We recently discovered that an eCB tone regulates neuroblast migration *in vitro* and *in vivo* (Oudin et al., 2011b). Stimulation of the CB1 receptor with the selective agonist arachidonyl-2'-chloroethylamide (ACEA) (Pertwee, 2006), which enhances neuroblast motility (Oudin et al., 2011b), significantly increased FRET efficiency levels for the GFP-fascin/PKCγ-RFP pair compared with vehicle-treated cells, indicating that fascin–PKC interaction can be modulated by cannabinoid signaling (Fig. 11). Importantly, this effect was abolished by preincubation with the selective CB1 receptor antagonist AM-251 (Pertwee, 2006), supporting its specific dependence on CB1 receptor activation. Interestingly, incubating cells only with AM-251 was sufficient to

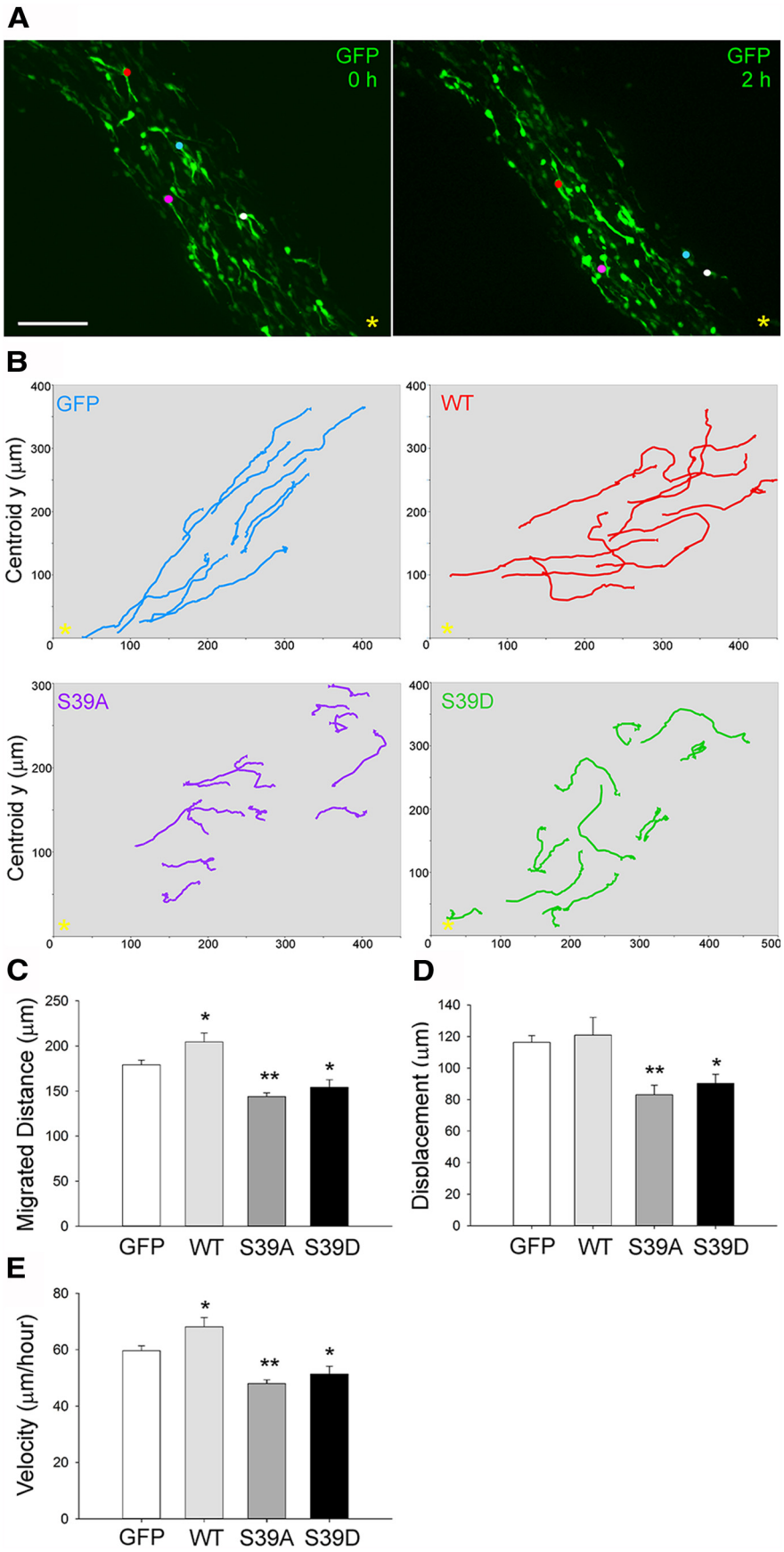

Figure 9. Phosphorylation of fascin on Ser39 regulates neuroblast migration *ex vivo*. ***A***, P2 mice were electroporated in the lateral ventricle with pGFPC2 (empty vector); pGFPC2-wt, -S39D, or -S39A fascin; and pCX-EGFP in a 3:1 ratio. Acute brain slices were prepared 5 d after electroporation. Projections of spinning disk confocal *z*-stack images (taken at times 0 and 2 h) from time-lapse microscopy showing GFP-expressing neuroblasts (colored dots) migrating toward the OB (yellow asterisk). ***B***, Neuroblasts expressing wt, S39A, or S39D fascin tend to display an enhanced exploratory behavior compared with control cells expressing only GFP, as shown here by some representative migratory paths from time-lapse imaging of brain slices over a period of 3 h. The yellow asterisk marks the location of the OB. ***C–E***, Based on quantitative tracking analysis, the expression of S39D or S39A fascin significantly decreases migrated distance, speed, and displacement, while wt fascin overexpression increases migration distance and speed (mean ± SEM; $n = 8$ slices for control; $n = 5$ slices for wt; and $n = 6$ slices for S39A and S39D; $^{*}p < 0.05$; $^{**}p < 0.01$). Scale bar, 85 μm.

significantly decrease fascin/PKC FRET efficiency levels, consistent with the existence of an endogenous cannabinoid tone in neuroblast cultures able to modulate the fascin–PKC interaction (Oudin et al., 2011b). Together, our results suggest that endogenous stimuli controlling neuroblast migration such as eCB signaling are able to regulate the interaction between fascin and PKC, thus contributing to achieve efficient cell motility.

Discussion

Here we provide several lines of evidence that fascin is required for proper migration of SVZ-derived neuroblasts. First, *fascin-1ko* mice display an abnormal RMS and a smaller OB compared with wt littermates. Second, both genetic deletion and siRNA-mediated depletion of fascin impair the migration of neuroblasts and disrupt their polarized morphology. Third, altering the phosphorylation state of fascin on Ser39 significantly decreases migration speed and affects directionality of movement, as shown by quantitative time-lapse imaging analysis of brain slices obtained from mice electroporated *in vivo*. Finally, our FLIM studies show that CB receptor signaling, which regulates neuroblast migration *in vivo*, is able to modulate the interaction between active PKC and Ser39-phosphorylated fascin.

Fascin regulates the polarized morphology of neuroblasts

Fascin has been implicated in neuronal morphogenesis and growth cone dynamics (Cohan et al., 2001; Kraft et al., 2006; Yamakita et al., 2009; Nagel et al., 2012). We have now discovered an additional function for fascin in migratory neuroblasts, where this protein is highly upregulated. Interestingly, some cytoskeleton-associated proteins, including fascin, are upregulated in human embryonic stem cell-derived neural progenitors (Chae et al., 2009),

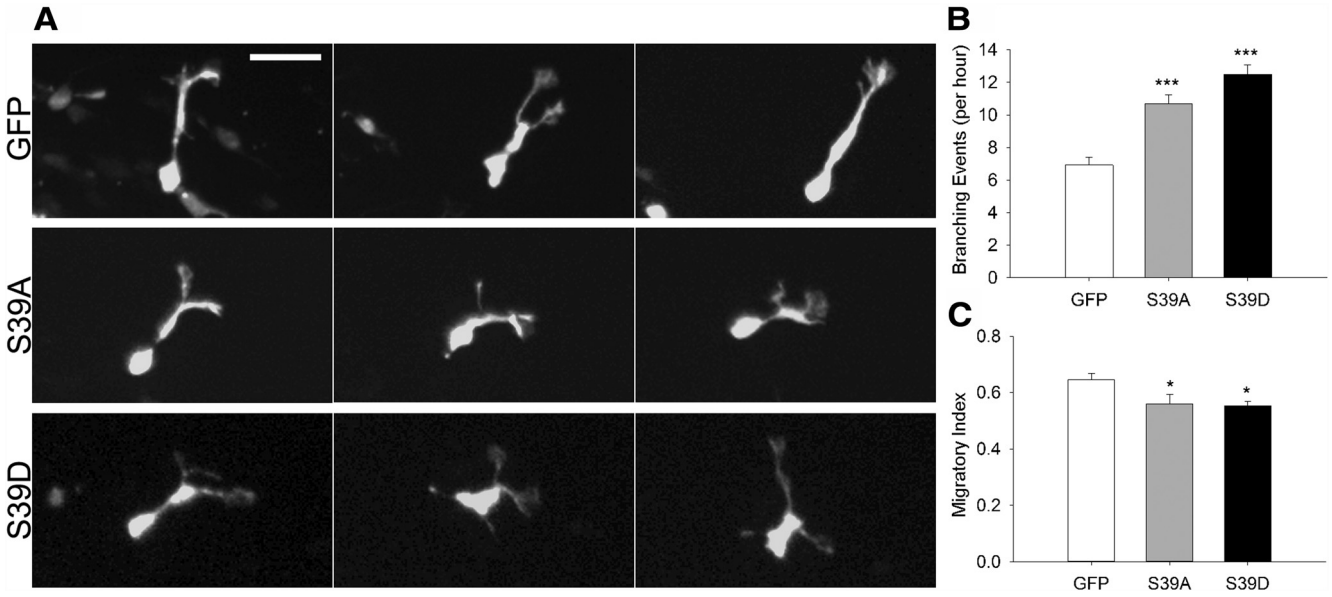

Figure 10. Phosphorylation of fascin on Ser39 regulates neuroblast directionality *ex vivo*. P2 mice were electroporated in the lateral ventricle with pGFPC2 (empty vector), pGFPC2-S39D or -S39A fascin, and pCX-EGFP in a 3:1 ratio. Acute brain slices were prepared 5 d after electroporation. ***A***, Projections of spinning disk confocal *z*-stacks (corresponding to the same cell imaged at three different time points) showing representative migrating neuroblasts expressing GFP, S39A fascin, or S39D fascin. Cells expressing S39A (middle row) or S39D (bottom row) fascin branched more frequently compared with GFP-expressing cells (top row). ***B***, Detailed analysis of spinning disk movies shows an increase in the number of branching events per hour for neuroblasts expressing S39A or S39D fascin compared with control cells (mean ± SEM; $n = 80$ cells from eight brain slices for GFP; and $n = 60$ cells from six brain slices for S39A and S39D; ***$p < 0.001$). ***C***, The migratory index (net distance divided by total distance) is significantly decreased by the expression of either S39A or S39D fascin (mean ± SEM; $n = 8$ slices for control; $n = 6$ slices each for S39A and S39D; *$p < 0.05$). Scale bar, 30 μm.

suggesting an important function for cytoskeletal reorganization in neural lineage differentiation. Consistent with a role in regulating cell motility in a stem cell context, fascin is one of the most upregulated targets in knock-out mice for the tuberous sclerosis complex component TSC1 promoting hematopoietic stem cell mobilization (Gan et al., 2008). Interestingly, TSC1 loss also affects neuroblast migration (Zhou et al., 2011; Feliciano et al., 2012). In the SVZ, fascin overlaps with Dcx+ neuroblasts, being excluded from ependymal cells and GFAP+ stem cells/astrocytes, and hardly detectable in Mash1+ progenitors. Fascin upregulation could therefore be considered a characteristic feature of migrating neuroblasts.

Fascin appears to regulate the polarized morphology of migratory neuroblasts since its depletion leads to branched processes (Fig. 5). In a parallel comparison, γ neurons mutant for *singed* (the fascin ortholog) in *Drosophila* mushroom bodies fail to maintain their straight trajectory (Kraft et al., 2006). This phenotype may be due to decreased lack of adhesiveness with the substrate. Attachment and detachment are critical steps in cell migration, and adhesion molecules such as active β1-integrin subunits are concentrated in the leading process of migrating neuroblasts (Shieh et al., 2011) and at filopodial tips in growth cones (Galbraith et al., 2007). Fascin, which we find particularly localized on protrusive filopodia at the neuroblast leading edge, may be involved in the fine local regulation of actin bundling. Nascent adhesions at the leading edge provide strong traction forces on the local ECM environment and on cell–cell contacts, which could be important for the development of polarized protrusions (Hashimoto et al., 2007). Such adhesion may be integrin based, given the presence of several integrin subunits in the SVZ/RMS and the requirement for β1-integrin in RMS neuroblast migration (Murase and Horwitz, 2002; Belvindrah et al., 2007; Kazanis et al., 2010). Moreover, genetic deletion of β1-integrin disrupts the morphology of neuroblasts, which display several leading processes free to explore the environment, similar to fascin depletion (Belvindrah et al., 2007). It would be interesting to examine whether fascin regulates integrin localization in neuroblasts, given that in other cell types fascin overexpression can stimulate migration by controlling the relocation of β1-integrin and vinculin, key players in adhesion to the ECM (Yamashiro et al., 1998; Jawhari et al., 2003) and that *in vivo* overexpression of fascin tends to increase neuroblast motility (Fig. 9).

The function of Ser39 phosphorylation

Our nucleofection and *in vivo* electroporation experiments with nonphosphorylatable and phosphomimetic fascin mutants strongly suggest that dynamic fascin phosphorylation on S39 is required for proper neuroblast morphology and motility. From early postnatal to adult stages, neuroblast chains progressively become surrounded by an astrocytic tunnel (Peretto et al., 2005). In addition, blood vessels topographically outlining the RMS provide molecular cues and a physical scaffold promoting neuroblast motility (Bovetti et al., 2007; Snapyan et al., 2009; Bozoyan et al., 2012). To move through such a complex environment, neuroblasts are likely to continuously reorganize their cytoskeleton and their adhesive properties, as shown by time-lapse imaging in this and other reports (Nam et al., 2007; Saha et al., 2012). Phosphorylation/dephosphorylation on S39 would favor the cycling of fascin on/off peripheral actin filaments, thus providing a dynamic control of actin bundling and at the same time modulating the balance between protrusions and adhesions. This mode of action would be analogous to the one observed in highly invasive cancer cells that, like neuroblasts, express high levels of fascin (Hashimoto et al., 2011). S39A and S39D mutants impaired migration in the Matrigel assay and in brain slice cultures derived from animals electroporated *in vivo*. Therefore, while the actin-bundling activity of nonphosphorylated fascin may be required for proper motility, localized events

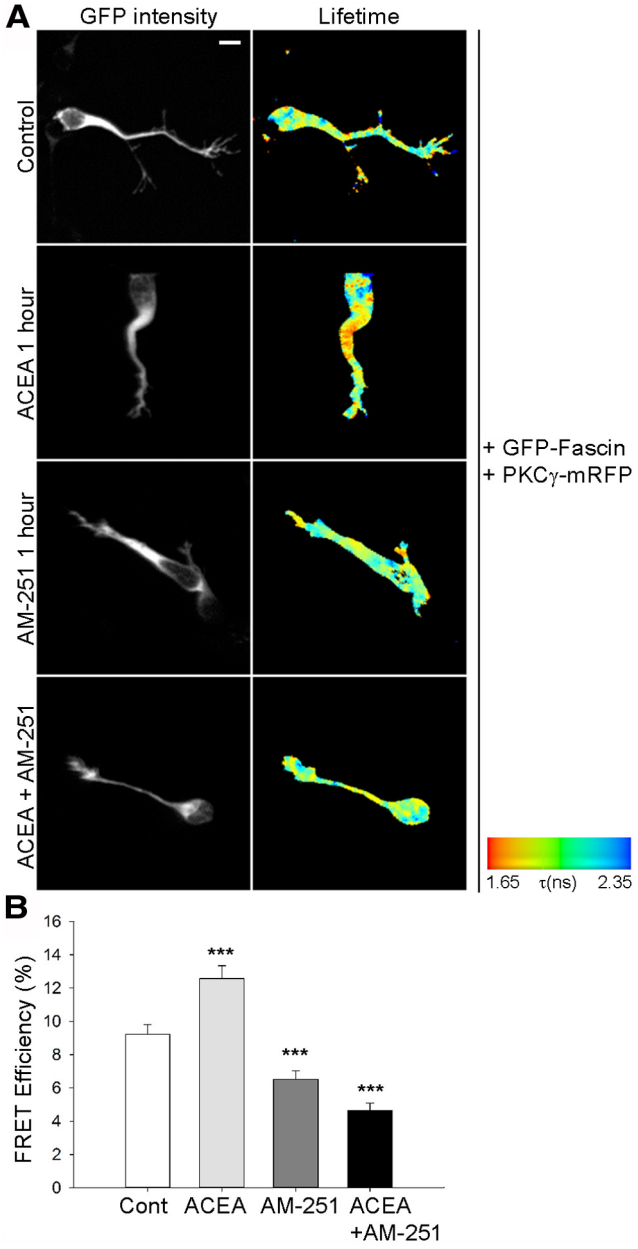

Figure 11. Cannabinoid signaling regulates the interaction between PKC and fascin. ***A***, Rat neuroblasts expressing GFP-fascin and PKCγ-mRFP were embedded in Matrigel 24 h after nucleofection, left to migrate for 9 h, and then treated with control (Cont) vehicle, the CB1 agonist ACEA (0.5 μM), or the CB1 antagonist AM-251 (0.5 μM) for 1 h. In a third experiment, cells were preincubated for 1 h with AM-251 before the addition of ACEA for 1 h to the medium. Cells were then fixed and imaged using FLIM to measure FRET efficiency. For each of these conditions, intensity multiphoton GFP images (donor) and pseudocolored lifetime images are shown. ***B***, Quantitative analysis of FRET efficiency shows that CB1 receptor activation by ACEA stimulates the PKC–fascin interaction, while preincubation with the CB1 receptor antagonist AM-251 prevents this effect. AM-251 on its own also significantly inhibits the PKC–fascin interaction, consistent with the presence of an endogenous cannabinoid tone in the culture (mean ± SEM; $n = 27$ cells for control; $n = 17$ cells for ACEA; $n = 19$ cells for AM-251; $n = 16$ cells for ACEA + AM-251, from three independent experiments; $^{***}p < 0.001$). Scale bar, 5 μm.

leading to PKC activation (e.g., integrin signaling) could downregulate the ability of fascin to cross-link actin filaments and promote the formation of a phospho-fascin/PKC complex, maintaining active PKC at appropriate subcellular locations to control adhesion. In line with this, overexpressing the phosphomimic S39D or S39A mutants would perturb the tightly regulated balance between phospho-and non-phospho fascin, leading to motility and misorientation defects. By binding to activated PKC, the S39D mutant could produce a dominant-negative effect (Hashimoto et al., 2011), similar to other experimental paradigms where S39D can compete for the endogenous interaction of PKC with fascin (Anilkumar et al., 2003). A recent study showed that another evolutionarily conserved phosphorylation residue (S289/274) in the C terminus of fascin may be important to regulate filopodial extension independent of actin-bundling activity (Zanet et al., 2012). In that report, it was suggested that fascin may be part of an adhesion-dependent complex that could help to modulate actin bundling. Whether phosphorylation on this residue also plays an active role in controlling neuroblast migration remains to be investigated.

Signals regulating fascin

In non-neuronal cells, several signals are able to regulate phosphorylation of fascin and its association with active PKC. These include a number of ECM components, such as thrombospondin-1, tenascin-C, and fibronectin, and cell adhesion molecules like syndecan-1 and integrins (Adams, 2004; Jayo and Parsons, 2010; Hashimoto et al., 2011). While thrombospondin/syndecan-1 and tenascin-C promote fascin-mediated actin bundling and protrusion stabilization, integrin signaling and fibronectin instead inhibit acting bundling and destabilize protrusions by promoting PKC-dependent phosphorylation of fascin on Ser39 (Kureishy et al., 2002; Adams, 2004). Interestingly, many of these fascin-regulating molecules are present along the RMS; for example, high syndecan-1 expression is found on migrating neuroblasts, while fibronectin is abundant around the blood vessels that facilitate their movement (Bovetti et al., 2007; Kazanis et al., 2010). Moreover, both thrombospondin-1 and β1-integrin knock-out mice display anatomical abnormalities of the RMS and a marked reduction of neural precursors entering the OB (Belvindrah et al., 2007; Blake et al., 2008). Therefore, a variety of signals in the RMS could participate in the intracellular dynamic regulation of fascin in neuroblasts, ultimately contributing to the proper arrival of neural precursors in the OB.

Fascin-1ko mice display cell accumulation in the caudal area of the RMS, suggesting impaired neuroblast exit from the SVZ. This phenotype is similar to the one reported for *IGF-1ko* mice (Hurtado-Chong et al., 2009). Interestingly, IGF appears to stimulate fascin-dependent protrusion in breast cancer cells (Guvakova et al., 2002), and in the same model syndecan-1 can potentiate FGF-2 signaling (Filla et al., 1998). Notably, FGF-2 appears to be present in a caudo–rostral gradient along the RMS and has been proposed to act as a motogenic cue feeding the migration of newly produced precursors at least in the early postnatal period (García-González et al., 2010). FGF and other factors have the ability to cross talk to the eCB signaling system, a fundamental player in CNS development (Williams et al., 2003; Harkany et al., 2008; Oudin et al., 2011a). We recently demonstrated that an endogenous cannabinoid tone controls the migration and morphology of RMS neuroblasts *in vivo* (Oudin et al., 2011b), and here we show that CB signaling can modulate the interaction between fascin and PKC in these cells. To understand how this contributes to efficient neuroblast migration it will be important to analyze the dynamic and spatial features of eCB-dependent effects on fascin/PKC interaction and identify the signaling intermediates involved, which could include local rises in intracellular calcium (Williams et al., 2003) or activation of the small GTPase Rac (Parsons and Adams, 2008).

In conclusion, we have shown that fascin is selectively upregulated in migratory neuroblasts of the postnatal SVZ niche and is required to ensure their correct migration toward the OB. Our *ex vivo* work highlights the importance of fascin phosphorylation on Ser39, a dynamic event that would allow a fine regulation of neuroblast motility according to the surrounding microenvironment. Based on our data, we propose that CB receptor activation and potentially other signals along the RMS modulate the interaction between active PKC and Ser39-phosphorylated fascin to control actin remodeling/PKC localization during polarized neuroblast migration. Since altering neuroblast motility affects neuronal maturation (Belvindrah et al., 2011), it will be interesting to explore the contribution of fascin to subsequent neurogenic steps, such as the acquisition of appropriate fate, differentiation and functional integration into pre-existing synaptic networks.

References

Adams JC (2004) Roles of fascin in cell adhesion and motility. Curr Opin Cell Biol 16:590–596. CrossRef Medline

Adams JC, Schwartz MA (2000) Stimulation of fascin spikes by thrombospondin-1 is mediated by the GTPases Rac and Cdc42. J Cell Biol 150:807–822. CrossRef Medline

Alvarez-Buylla A, Lim DA (2004) For the long run: maintaining germinal niches in the adult brain. Neuron 41:683–686. CrossRef Medline

Anilkumar N, Parsons M, Monk R, Ng T, Adams JC (2003) Interaction of fascin and protein kinase Calpha: a novel intersection in cell adhesion and motility. EMBO J 22:5390–5402. CrossRef Medline

Bagley JA, Belluscio L (2010) Dynamic imaging reveals that brain-derived neurotrophic factor can independently regulate motility and direction of neuroblasts within the rostral migratory stream. Neuroscience 169:1449–1461. CrossRef Medline

Belvindrah R, Hankel S, Walker J, Patton BL, Müller U (2007) β1 integrins control the formation of cell chains in the adult rostral migratory stream. J Neurosci 27:2704–2717. CrossRef Medline

Belvindrah R, Nissant A, Lledo PM (2011) Abnormal neuronal migration changes the fate of developing neurons in the postnatal olfactory bulb. J Neurosci 31:7551–7562. CrossRef Medline

Blake SM, Strasser V, Andrade N, Duit S, Hofbauer R, Schneider WJ, Nimpf J (2008) Thrombospondin-1 binds to ApoER2 and VLDL receptor and functions in postnatal neuronal migration. EMBO J 27:3069–3080. CrossRef Medline

Boutin C, Diestel S, Desoeuvre A, Tiveron MC, Cremer H (2008) Efficient in vivo electroporation of the postnatal rodent forebrain. PLoS One 3:e1883. CrossRef Medline

Bovetti S, Hsieh YC, Bovolin P, Perroteau I, Kazunori T, Puche AC (2007) Blood vessels form a scaffold for neuroblast migration in the adult olfactory bulb. J Neurosci 27:5976–5980. CrossRef Medline

Bozoyan L, Khlghatyan J, Saghatelyan A (2012) Astrocytes control the development of the migration-promoting vasculature scaffold in the postnatal brain via VEGF signaling. J Neurosci 32:1687–1704. CrossRef Medline

Brown JA, Bridgman PC (2009) Disruption of the cytoskeleton during Semaphorin 3A induced growth cone collapse correlates with differences in actin organization and associated binding proteins. Dev Neurobiol 69:633–646. CrossRef Medline

Chae JI, Kim J, Woo SM, Han HW, Cho YK, Oh KB, Nam KH, Kang YK (2009) Cytoskeleton-associated proteins are enriched in human embryonic-stem cell-derived neuroectodermal spheres. Proteomics 9:1128–1141. CrossRef Medline

Chazal G, Durbec P, Jankovski A, Rougon G, Cremer H (2000) Consequences of neural cell adhesion molecule deficiency on cell migration in the rostral migratory stream of the mouse. J Neurosci 20:1446–1457. Medline

Cohan CS, Welnhofer EA, Zhao L, Matsumura F, Yamashiro S (2001) Role of the actin bundling protein fascin in growth cone morphogenesis: localization in filopodia and lamellipodia. Cell Motil Cytoskeleton 48:109–120. CrossRef Medline

Comte I, Kim Y, Young CC, van der Harg JM, Hockberger P, Bolam PJ, Poirier F, Szele FG (2011) Galectin-3 maintains cell motility from the subventricular zone to the olfactory bulb. J Cell Sci 124:2438–2447. CrossRef Medline

Conover JC, Doetsch F, Garcia-Verdugo JM, Gale NW, Yancopoulos GD, Alvarez-Buylla A (2000) Disruption of Eph/ephrin signaling affects migration and proliferation in the adult subventricular zone. Nat Neurosci 3:1091–1097. CrossRef Medline

Curtis MA, Eriksson PS, Faull RL (2007) Progenitor cells and adult neurogenesis in neurodegenerative diseases and injuries of the basal ganglia. Clin Exp Pharmacol Physiol 34:528–532. CrossRef Medline

De Arcangelis A, Georges-Labouesse E, Adams JC (2004) Expression of fascin-1, the gene encoding the actin-bundling protein fascin-1, during mouse embryogenesis. Gene Expr Patterns 4:637–643. CrossRef Medline

Deinhardt K, Kim T, Spellman DS, Mains RE, Eipper BA, Neubert TA, Chao MV, Hempstead BL (2011) Neuronal growth cone retraction relies on proneurotrophin receptor signaling through Rac. Sci Signal 4:ra82. CrossRef Medline

Doetsch F, Caillé I, Lim DA, García-Verdugo JM, Alvarez-Buylla A (1999) Subventricular zone astrocytes are neural stem cells in the adult mammalian brain. Cell 97:703–716. CrossRef Medline

Feliciano DM, Quon JL, Su T, Taylor MM, Bordey A (2012) Postnatal neurogenesis generates heterotopias, olfactory micronodules and cortical infiltration following single-cell Tsc1 deletion. Hum Mol Genet 21:799–810. CrossRef Medline

Filla MS, Dam P, Rapraeger AC (1998) The cell surface proteoglycan syndecan-1 mediates fibroblast growth factor-2 binding and activity. J Cell Physiol 174:310–321. CrossRef Medline

Galbraith CG, Yamada KM, Galbraith JA (2007) Polymerizing actin fibers position integrins primed to probe for adhesion sites. Science 315:992–995. CrossRef Medline

Gan B, Sahin E, Jiang S, Sanchez-Aguilera A, Scott KL, Chin L, Williams DA, Kwiatkowski DJ, DePinho RA (2008) mTORC1-dependent and -independent regulation of stem cell renewal, differentiation, and mobilization. Proc Natl Acad Sci U S A 105:19384–19389. CrossRef Medline

García-González D, Clemente D, Coelho M, Esteban PF, Soussi-Yanicostas N, de Castro F (2010) Dynamic roles of FGF-2 and anosmin-1 in the migration of neuronal precursors from the subventricular zone during pre- and postnatal development. Exp Neurol 222:285–295. CrossRef Medline

Goncalves MB, Suetterlin P, Yip P, Molina-Holgado F, Walker DJ, Oudin MJ, Zentar MP, Pollard S, Yáñez-Muñoz RJ, Williams G, Walsh FS, Pangalos MN, Doherty P (2008) A diacylglycerol lipase-CB2 cannabinoid pathway regulates adult subventricular zone neurogenesis in an age-dependent manner. Mol Cell Neurosci 38:526–536. CrossRef Medline

Guvakova MA, Boettiger D, Adams JC (2002) Induction of fascin spikes in breast cancer cells by activation of the insulin-like growth factor-I receptor. Int J Biochem Cell Biol 34:685–698. CrossRef Medline

Harkany T, Mackie K, Doherty P (2008) Wiring and firing neuronal networks: endocannabinoids take center stage. Curr Opin Neurobiol 18:338–345. CrossRef Medline

Hashimoto Y, Parsons M, Adams JC (2007) Dual actin-bundling and protein kinase C-binding activities of fascin regulate carcinoma cell migration downstream of Rac and contribute to metastasis. Mol Biol Cell 18:4591–4602. CrossRef Medline

Hashimoto Y, Kim DJ, Adams JC (2011) The roles of fascins in health and disease. J Pathol 224:289–300. CrossRef Medline

Hirota Y, Ohshima T, Kaneko N, Ikeda M, Iwasato T, Kulkarni AB, Mikoshiba K, Okano H, Sawamoto K (2007) Cyclin-dependent kinase 5 is required for control of neuroblast migration in the postnatal subventricular zone. J Neurosci 27:12829–12838. CrossRef Medline

Hurtado-Chong A, Yusta-Boyo MJ, Vergaño-Vera E, Bulfone A, de Pablo F, Vicario-Abejón C (2009) IGF-I promotes neuronal migration and positioning in the olfactory bulb and the exit of neuroblasts from the subventricular zone. Eur J Neurosci 30:742–755. CrossRef Medline

Jawhari AU, Buda A, Jenkins M, Shehzad K, Sarraf C, Noda M, Farthing MJ, Pignatelli M, Adams JC (2003) Fascin, an actin-bundling protein, modulates colonic epithelial cell invasiveness and differentiation in vitro. Am J Pathol 162:69–80. CrossRef Medline

Jayo A, Parsons M (2010) Fascin: a key regulator of cytoskeletal dynamics. Int J Biochem Cell Biol 42:1614–1617. CrossRef Medline

Jayo A, Parsons M, Adams JC (2012) A novel Rho-dependent pathway that drives interaction of fascin-1 with p-Lin-11/Isl-1/Mec-3 kinase (LIMK)

1/2 to promote fascin-1/actin binding and filopodia stability. BMC Biol 10:72. CrossRef Medline

Kaneko N, Marín O, Koike M, Hirota Y, Uchiyama Y, Wu JY, Lu Q, Tessier-Lavigne M, Alvarez-Buylla A, Okano H, Rubenstein JL, Sawamoto K (2010) New neurons clear the path of astrocytic processes for their rapid migration in the adult brain. Neuron 67:213–223. CrossRef Medline

Kazanis I, Lathia JD, Vadakkan TJ, Raborn E, Wan R, Mughal MR, Eckley DM, Sasaki T, Patton B, Mattson MP, Hirschi KK, Dickinson ME, ffrench-Constant C (2010) Quiescence and activation of stem and precursor cell populations in the subependymal zone of the mammalian brain are associated with distinct cellular and extracellular matrix signals. J Neurosci 30:9771–9781. CrossRef Medline

Koizumi H, Higginbotham H, Poon T, Tanaka T, Brinkman BC, Gleeson JG (2006) Doublecortin maintains bipolar shape and nuclear translocation during migration in the adult forebrain. Nat Neurosci 9:779–786. CrossRef Medline

Kraft R, Escobar MM, Narro ML, Kurtis JL, Efrat A, Barnard K, Restifo LL (2006) Phenotypes of *Drosophila* brain neurons in primary culture reveal a role for fascin in neurite shape and trajectory. J Neurosci 26:8734–8747. CrossRef Medline

Kureishy N, Sapountzi V, Prag S, Anilkumar N, Adams JC (2002) Fascins, and their roles in cell structure and function. Bioessays 24:350–361. CrossRef Medline

Li A, Dawson JC, Forero-Vargas M, Spence HJ, Yu X, König I, Anderson K, Machesky LM (2010) The actin-bundling protein fascin stabilizes actin in invadopodia and potentiates protrusive invasion. Curr Biol 20: 339–345. CrossRef Medline

Lledo PM, Alonso M, Grubb MS (2006) Adult neurogenesis and functional plasticity in neuronal circuits. Nat Rev Neurosci 7:179–193. CrossRef Medline

Lois C, Alvarez-Buylla A (1994) Long-distance neuronal migration in the adult mammalian brain. Science 264:1145–1148. CrossRef Medline

Luskin MB (1993) Restricted proliferation and migration of postnatally generated neurons derived from the forebrain subventricular zone. Neuron 11:173–189. CrossRef Medline

Murase S, Horwitz AF (2002) Deleted in colorectal carcinoma and differentially expressed integrins mediate the directional migration of neural precursors in the rostral migratory stream. J Neurosci 22:3568–3579. Medline

Nagel J, Delandre C, Zhang Y, Förstner F, Moore AW, Tavosanis G (2012) Fascin controls neuronal class-specific dendrite arbor morphology. Development 139:2999–3009. CrossRef Medline

Nam SC, Kim Y, Dryanovski D, Walker A, Goings G, Woolfrey K, Kang SS, Chu C, Chenn A, Erdelyi F, Szabo G, Hockberger P, Szele FG (2007) Dynamic features of postnatal subventricular zone cell motility: a two-photon time-lapse study. J Comp Neurol 505:190–208. CrossRef Medline

Nguyen-Ba-Charvet KT, Plump AS, Tessier-Lavigne M, Chedotal A (2002) Slit1 and slit2 proteins control the development of the lateral olfactory tract. J Neurosci 22:5473–5480. Medline

Ono S, Yamakita Y, Yamashiro S, Matsudaira PT, Gnarra JR, Obinata T, Matsumura F (1997) Identification of an actin binding region and a protein kinase C phosphorylation site on human fascin. J Biol Chem 272:2527–2533. CrossRef Medline

Oudin MJ, Hobbs C, Doherty P (2011a) DAGL-dependent endocannabinoid signalling: roles in axonal pathfinding, synaptic plasticity and adult neurogenesis. Eur J Neurosci 34:1634–1646. CrossRef Medline

Oudin MJ, Gajendra S, Williams G, Hobbs C, Lalli G, Doherty P (2011b) Endocannabinoids regulate the migration of subventricular zone-derived neuroblasts in the postnatal brain. J Neurosci 31:4000–4011. CrossRef Medline

Parsons M, Adams JC (2008) Rac regulates the interaction of fascin with protein kinase C in cell migration. J Cell Sci 121:2805–2813. CrossRef Medline

Parsons M, Vojnovic B, Ameer-Beg S (2004) Imaging protein-protein interactions in cell motility using fluorescence resonance energy transfer (FRET). Biochem Soc Trans 32:431–433. CrossRef Medline

Pathania M, Yan LD, Bordey A (2010) A symphony of signals conducts early and late stages of adult neurogenesis. Neuropharmacology 58:865–876. CrossRef Medline

Peretto P, Giachino C, Aimar P, Fasolo A, Bonfanti L (2005) Chain formation and glial tube assembly in the shift from neonatal to adult subventricular zone of the rodent forebrain. J Comp Neurol 487:407–427. CrossRef Medline

Pertwee RG (2006) The pharmacology of cannabinoid receptors and their ligands: an overview. Int J Obes (Lond) 30 [Suppl 1]:S13–S18. CrossRef Medline

Saha B, Ypsilanti AR, Boutin C, Cremer H, Chédotal A (2012) Plexin-b2 regulates the proliferation and migration of neuroblasts in the postnatal and adult subventricular zone. J Neurosci 32:16892–16905. CrossRef Medline

Sanai N, Nguyen T, Ihrie RA, Mirzadeh Z, Tsai HH, Wong M, Gupta N, Berger MS, Huang E, Garcia-Verdugo JM, Rowitch DH, Alvarez-Buylla A (2011) Corridors of migrating neurons in the human brain and their decline during infancy. Nature 478:382–386. CrossRef Medline

Sawamoto K, Wichterle H, Gonzalez-Perez O, Cholfin JA, Yamada M, Spassky N, Murcia NS, Garcia-Verdugo JM, Marin O, Rubenstein JL, Tessier-Lavigne M, Okano H, Alvarez-Buylla A (2006) New neurons follow the flow of cerebrospinal fluid in the adult brain. Science 311: 629–632. CrossRef Medline

Shieh JC, Schaar BT, Srinivasan K, Brodsky FM, McConnell SK (2011) Endocytosis regulates cell soma translocation and the distribution of adhesion proteins in migrating neurons. PLoS One 6:e17802. CrossRef Medline

Shinohara R, Thumkeo D, Kamijo H, Kaneko N, Sawamoto K, Watanabe K, Takebayashi H, Kiyonari H, Ishizaki T, Furuyashiki T, Narumiya S (2012) A role for mDia, a Rho-regulated actin nucleator, in tangential migration of interneuron precursors. Nat Neurosci 15:373–380, S1–S2. CrossRef Medline

Snapyan M, Lemasson M, Brill MS, Blais M, Massouh M, Ninkovic J, Gravel C, Berthod F, Götz M, Barker PA, Parent A, Saghatelyan A (2009) Vasculature guides migrating neuronal precursors in the adult mammalian forebrain via brain-derived neurotrophic factor signaling. J Neurosci 29: 4172–4188. CrossRef Medline

Vignjevic D, Yarar D, Welch MD, Peloquin J, Svitkina T, Borisy GG (2003) Formation of filopodia-like bundles in vitro from a dendritic network. J Cell Biol 160:951–962. CrossRef Medline

Vignjevic D, Kojima S, Aratyn Y, Danciu O, Svitkina T, Borisy GG (2006) Role of fascin in filopodial protrusion. J Cell Biol 174:863–875. CrossRef Medline

Ward ME, Rao Y (2005) Investigations of neuronal migration in the central nervous system. Methods Mol Biol 294:137–156. Medline

Wichterle H, Garcia-Verdugo JM, Alvarez-Buylla A (1997) Direct evidence for homotypic, glia-independent neuronal migration. Neuron 18:779–791. CrossRef Medline

Williams EJ, Walsh FS, Doherty P (2003) The FGF receptor uses the endocannabinoid signaling system to couple to an axonal growth response. J Cell Biol 160:481–486. CrossRef Medline

Worth DC, Parsons M (2010) Advances in imaging cell-matrix adhesions. J Cell Sci 123:3629–3638. CrossRef Medline

Yamakita Y, Ono S, Matsumura F, Yamashiro S (1996) Phosphorylation of human fascin inhibits its actin binding and bundling activities. J Biol Chem 271:12632–12638. CrossRef Medline

Yamakita Y, Matsumura F, Yamashiro S (2009) Fascin1 is dispensable for mouse development but is favorable for neonatal survival. Cell Motil Cytoskeleton 66:524–534. CrossRef Medline

Yamashiro S, Yamakita Y, Ono S, Matsumura F (1998) Fascin, an actin-bundling protein, induces membrane protrusions and increases cell motility of epithelial cells. Mol Biol Cell 9:993–1006. Medline

Zanet J, Stramer B, Millard T, Martin P, Payre F, Plaza S (2009) Fascin is required for blood cell migration during Drosophila embryogenesis. Development 136:2557–2565. CrossRef Medline

Zanet J, Jayo A, Plaza S, Millard T, Parsons M, Stramer B (2012) Fascin promotes filopodia formation independent of its role in actin bundling. J Cell Biol 197:477–486. CrossRef Medline

Zhang H, Vutskits L, Pepper MS, Kiss JZ (2003) VEGF is a chemoattractant for FGF-2-stimulated neural progenitors. J Cell Biol 163:1375–1384. CrossRef Medline

Zhou J, Shrikhande G, Xu J, McKay RM, Burns DK, Johnson JE, Parada LF (2011) Tsc1 mutant neural stem/progenitor cells exhibit migration deficits and give rise to subependymal lesions in the lateral ventricle. Genes Dev 25:1595–1600. CrossRef Medline